CHALMERS

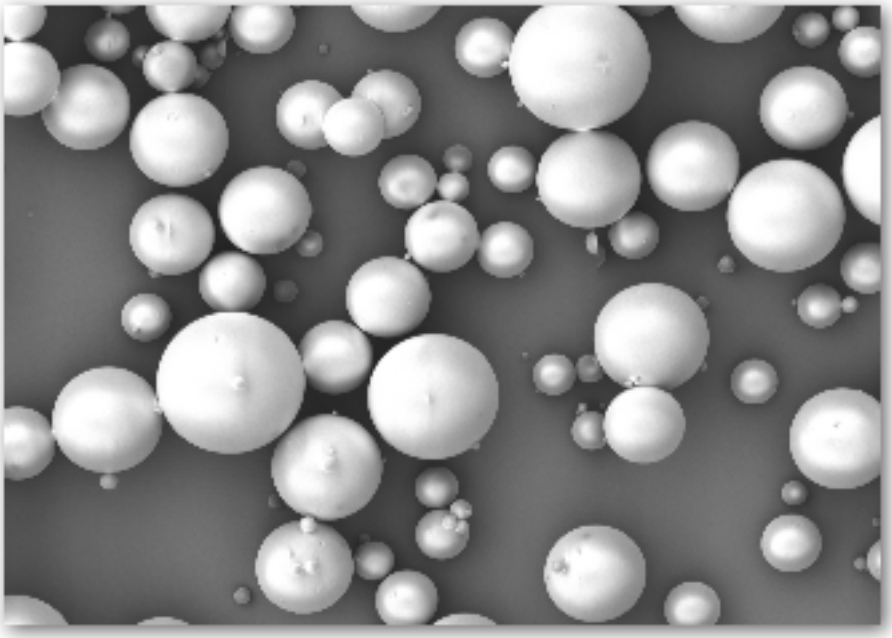

Gelation of colloidal silica sols

Master of Science Thesis

KATARINA RISÖ

Department of Chemical and Biological Engineering
Division of Applied Surface Chemistry
CHALMERS UNIVERSITY OF TECHNOLOGY
Göteborg, Sweden, 2011

Gelation of colloidal silica sols

KATARINA RISÖ

Department of Chemical and Biological Engineering
CHALMERS UNIVERSITY OF TECHNOLOGY
Göteborg, Sweden, 2011

Gelation of colloidal silica sols
KATARINA RISÖ

Department of Chemical and Biological Engineering
Chalmers University of Technology
SE-412 96 Göteborg
Sweden
Telephone +46 (0)31-772 1000

Cover: SEM image of spherical silica gel particles from pilot scale experiment

Chalmers Reproservice
Göteborg, Sweden 2011

Gelation of colloidal silica sols
KATARINA RISÖ
Department of Chemical and Biological Engineering
Chalmers University of Technology

Abstract

Silica is one of the most used column packing material for normal- and reversed phase liquid chromatography (LC). Porous perfectly spherical silica gel particles for high performance liquid chromatography (HPLC) can be produced by a sol-gel process in which a colloidal silica sol is dispersed in an oil phase and subsequently gelled.

The aim of this master thesis project was to study new methods to emulsify and gel colloidal silica sols and to use new grades of silica sols in the sol-gel step. The new methods of emulsification were membrane emulsification and static mixing emulsification. Particle sizes of 50 µm and 2 µm respectively for the two methods were desired. Four different sols were gelled in attempts to produce particles with a high specific surface area.

Particles with an average diameter of 41.4 µm were produced in a pilot scale reactor using the membrane emulsification method. The static mixing emulsification method was promising but the pressure limit of the used set-up interrupted the experimental series and the lowest average diameter achieved was 8.3 µm. A pilot scale experiment with stirring as emulsification method was performed and particles with an average diameter of 3.8 µm was produced. No significant increase in specific surface area was reached in the gelling experiments with different sols and more experiments needs to be performed before any conclusions can be drawn about this.

Keywords: Silica, Sols, Emulsification, Gelation, Chromatography

Contents

1 Introduction

Silica is one of the most used column packing material for normal- and reversed phase liquid chromatography (LC).

Separation Products, a sub-business unit of Eka Chemicals AB, is a leading manufacturer of materials for high performance liquid chromatography (HPLC). The materials are used in preparative chromatography for the purification of pharmaceuticals as well as for analytical separations in HPLC columns. The backbone of the materials is porous silica which is modified with different chemical functionalities to provide a resulting material with the desired separation properties.

The manufacturing process is highly complex and comprises many separate process steps. A sol-gel process is used to make perfectly spherical porous silica particles by emulsification of a colloidal silica sol in an organic phase. The emulsion droplets are gelled into solid porous particles which are then further processed in a number of subsequent process steps. Some of the most important physical properties of the resulting products are determined by the conditions used in the sol-gel step.

For Separation Products to be able to reach new markets in the future, more knowledge about how to control emulsification and gelation in the sol-gel step is required. The aim of this master thesis project was to study new methods to emulsify and gel colloidal silica sols and to use new grades of silica sols in the sol-gel step. Properties that were going to be investigated was specific surface area, specific pore volume (particle porosity) and particle size

The objective was to investigate different methods for preparing new chromatographic materials which exhibit different physical properties than the existing products. Three main tasks were decided upon. First, production of spherical silica gel particles using a version of membrane emulsification was to be tested. The produced particles should preferably have a fairly narrow size distribution to give as high yield of material with a size around 50 µm as possible. The second task was to produce small particles and investigate if a static-mixer setup could be used for this purpose. Here a high yield of particles with a diameter of 2 µm was desired. The third task was to gel different silica sols to investigate if a higher specific surface area of the resulting material could be obtained.

The scope of the work was to prepare porous silica materials by using a sol-gel process. Procedures for packing materials in columns and subsequent chromatographic evaluation were to be made by staff at Separation Products, and were not a part of this work.

The theory part of this report covers the basics in silica gel production and sol-gel sciences together with some theory about membrane emulsification and static mixing properties. The measuring methods used to characterize the produces samples will also be described properly.

The experimental work is rather empirical in its nature since no earlier research on these methods has been performed on this particular system. The method part of the report includes the experimental setups and procedures. The experiments for the different tasks have not been performed in a specific order as the regents, reactors and operators needed to execute the experiments have been prioritised for the normal production at Separation Products.

2 Silica gel for HPLC

Silica, short for silicon dioxide, is the most widely used material in normal- and reversed-phase liquid chromatography (LC). It has the general formula $SiO_2 \cdot xH_2O$, where the water is chemically bound in a non-stoichiometric amount forming silanol groups (Si−OH), which are essential for making stationary phases for HPLC [1]. The surface silanols themselves give the packing a polar character which is used in normal-phase LC. To obtain a bonded phase the silanols are used to graft organic moieties [1]. The chromatographic properties of silica and the chemistry of silica are extensively described by Unger [2] and Iler [3].

There are several different types of silica packings in use [2]. The focus of this theoretical part will be on completely porous, non-crystalline, spherical gel particles similar to the ones produced at the division Separation Products at Eka chemicals AB under the brand name Kromasil.

2.1 Silica sol-gel science

According to Iler [3] the formation of silica gel can be regarded as taking place in two stages. First, colloidal silica sol particles are formed through polymerisation of silicic acid, $Si(OH)_4$, in aqueous solution. Next step is the actual gelling step; here the primary particles condense together and form a very open but continuous structure which extends throughout the medium. Both stages of polymerisation comprise a condensation reaction forming Si−O−Si linkages, siloxane bonds. The main difference between the two stages is that in the first step, condensation leads to particles of massive silica while in the second step the number of siloxane bonds between the sol particles is smaller due to the limited fit of the common face, resulting in a rigid and highly porous structure.

The growth of primary particles occurs by an Oswald ripening mechanism, which means that particles grow in size and decrease in number as the more soluble small particles dissolve and reprecipitate on larger, less soluble particles [4]. It follows that the particle growth depends on the solubility of amorphous silica, which in turn primarily depends on pH and temperature [3], see figure 1a and 1b. From pH 2 to pH 8 the solubility decreases slightly, starting around 150 ppm, but increases rapidly after pH 8. The solubility of amorphous silica increases with temperature. Since primary particle growth occurs by Oswald ripening, the growth rate is also dependent on the particle size distribution [4].

In [3] by Iler, some indications of particle size under above mentioned different conditions are given. The higher solubility of the smaller particles discussed above applies for particles smaller than about 5 nm and is very pronounced when the size is less than 3 nm. Above pH 7, where the rate of dissolution and deposition of silica is high, particle growth continues at ordinary temperature until the particles are 5-10 nm in diameter. At low pH, where the rate of polymerisation and depolymerisation is slower, particle growth becomes negligible after a size of 2-4 nm. Higher temperatures lead to larger particle sizes, especially above pH 7.

In gel formation, the basic mechanisms are the collision of two silica particles and the formation of siloxane bonds to hold the particles together irreversibly. The

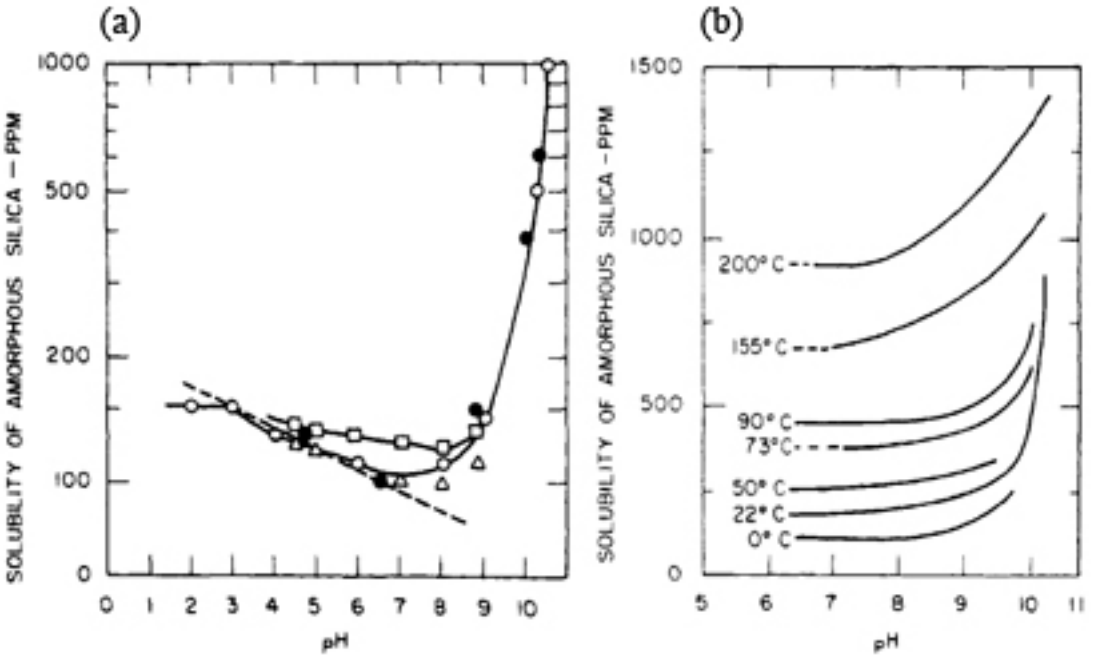

Figure 1: (a) Solubility of amorphous silica versus pH [3], (b) Solubility of amorphous silica versus pH at different temperatures [3]

siloxane bond formation is both acid and base catalysed depending on the charge of the particle [3]. For the collisions to occur, the particles need to have a sufficiently low surface charge due to electrostatic repulsion. Both reaction and collision rates are hence strongly affected by pH. The gelling is also affected by salt concentration, silica concentration and temperature. The temperature dependence is simple and is due to the kinetic phenomenon involved in aggregation, therefore the rate of gelling increases with temperature. Figure 2 shows an overview of the more complex effects of pH and salt concentration.

Since the condensation reaction for siloxane bond formation involves an ionic mechanism the reaction mechanism will be different depending on how the pH of the sol relates to the point of zero charge (PZC) and the isoelectric point (IEP) of silica. The PZC and IEP are both found around pH 2 and this region will hence be meta stable [3].

Above pH 2 the reaction is catalysed by hydroxyl ions and the reaction rate is proportional to the concentration of hydroxyl ions [3], as in eq 1 and eq 2.

$$\equiv \mathrm{Si{-}OH} + \mathrm{OH^-} \longrightarrow \equiv \mathrm{Si{-}O^-} + \mathrm{H_2O} \tag{1}$$

$$\equiv \mathrm{Si{-}O^-} + \mathrm{HO{-}Si^-} \longrightarrow \equiv \mathrm{Si{-}O{-}Si} + \mathrm{OH^-} \tag{2}$$

Below pH 2, the reaction rate is instead proportional to the H^+ concentration. Several different mechanisms for this reaction have been proposed [3, 4].

Above pH 6, the scarcity of hydroxyl ions is no longer the limiting factor for the rate of gelling. Instead, the rate of aggregation decreases because of fewer collisions

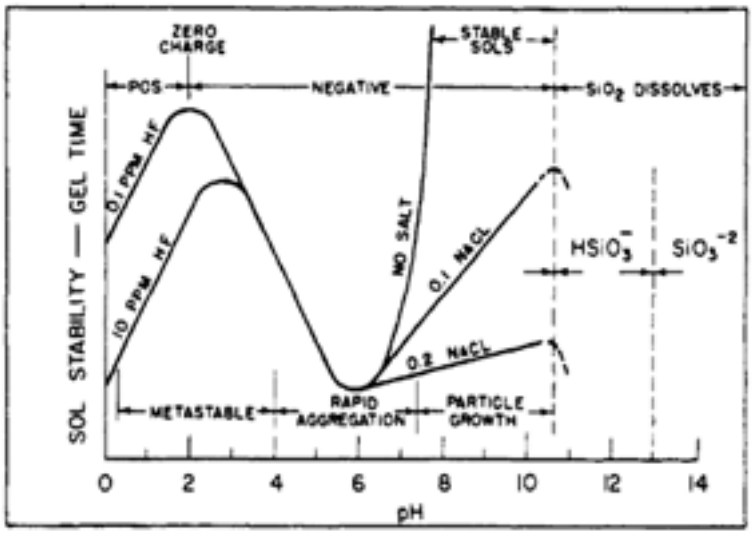

Figure 2: Effect of pH in the colloidal silica-water system [3]

between particles owing to the increasing charge on the particles. In this pH region the addition of salt reduces the gel time dramatically by reducing the thickness of the electrical double layer of the particles [4].

According to Iler [3], the rate of gelling appears to be proportional to the total area of silica surface present in a given volume of sol. This means that sols having the same ratio of concentration to particle diameter gel at about the same rate. Thus, under equivalent conditions, a 10% sol of 10 nm particles might be expected to gel at the same rate as a 20% sol of 20 nm particles.

The physico-chemical properties of the silica gel, which will be discussed in further detail in section 2.3, depend on the size of the primary particles. An increase in primary particle size leads to a decrease in specific surface area and an increase in porosity [1]. A balance between these properties is often desired to get a gel with a certain function.

In [1], Berthod points out the importance of know-how in silica-based LC packing preparation due to the crucial effect of pH and salt concentration on the final porous silica particles. As an example, he mentions a sodium silicate sol with a pH of around 12. If the pH is gently lowered to 10 the produced primary particles are 100 times larger than if the pH is rapidly lowered to 7. Each manufacturer has developed their own skills to prepare porous silica with the required particle size, specific surface area, pore volume, pore size and pore size distribution.

2.2 Production of spherical silica gel particles

Perfectly spherical silica particles for LC packing are often prepared by subdividing a colloidal silica sol into fine droplets before gelling [1]. This can be done in different ways including emulsification and spraying. When emulsification is used, one possible procedure is the one used in this study. This method will be described in further detail below.

The starting material is a colloidal silica sol with a known specific surface area, controlled by heat treatment. The sol is dispersed in an organic medium, immiscible with water, in the presence of a surface active agent to form an emulsion. The size of the formed droplets determines the size of the gel particles formed. A gelling process of the formed sol droplets takes place when water is evaporated under controlled temperature or when a salt is added to the emulsion. The particles are separated from the continuous phase and washed with an alcohol. To remove all organic material and make the gel particles stronger a heat treatment step called calcination is necessary. Due to the high temperature during the calcination many of the surface silanols form siloxane bridges which makes the surface of the gel particles more hydrophobic. A rehydroxylation step brings the silanol groups back.

2.2.1 Emulsification

Emulsions are dispersed systems of two immiscible liquids. The two phases are referred to as the dispersed phase (droplets) and the continuous phase. Almost all emulsions consist of a water phase and an organic phase. The emulsion is named depending on which phase that is the dispersed and the continuous, oil-in-water (o/w) or water-in-oil (w/o) emulsions. The system with colloidal silica sol as dispersed phase is consequently a water-in-oil emulsion.

Emulsification is the process of droplet formation. In [5], Peters describes droplet formation and the processes causing it. Droplets are formed by stress being imparted to a large primary drop. The stress causes elongation of the drop followed by development of surface waves. When the waves have grown to the point of instability the primary drop breaks into droplets and usually also smaller satellite droplets. In order to produce drops of the dispersed phase, the surface separating the two bulk phases must be disrupted. This can be achieved via turbulent eddies, surface ripples, Rayleigh-Taylor instabilities and Kelvin-Helmholtz instabilities. The two latter are caused by differences in density and velocity between the bulk phase and the dispersed phase. The process that is most easily modified in an existing system is the turbulent eddies by changing the mixing conditions. According to Groeneweg [6] there are two distinguished mechanisms for droplet break-up in turbulent flow: viscosity dominated break-up and inertia dominated break-up. Which one of these that is most relevant in a certain situation depends on the relation between the size of the largest drop and the length and the so called Kolmogorv eddies. Turbulent flow form large eddies which in turn creates smaller eddies with increased rotation, due to the conservation of angular momentum. The smallest eddies produced are called Kolmogorv eddies. If the maximum droplet diameter is small in comparison with the length scale of the Kolmogorv eddy the droplet break-up will occur by viscous forces. The viscous forces try to deform the droplets but are opposed by interfacial forces that try to maintain a spherical shape of the droplet. The ratio of these viscous forces and interfacial forces gives a dimensionless number; this number is by Peters [5] called the drop Weber number and by Groeneweg [6] the capillary number, Ω. The interfacial forces are of the order σ/R, where σ is the interfacial tension and R is the droplet radius. The viscous forces of the order $\dot{\gamma}\eta_c$ where $\dot{\gamma}$ is the shear rate (s^{-1}) and η_c is the dynamic viscosity of the continuous phase. The

equation for the capillary number is shown in eq 3.

$$\Omega = \dot{\gamma}\eta_c R/\sigma \tag{3}$$

If the capillary number Ω is larger than a critical value, drop break-up will occur. The critical value depends on the viscosity ratio of the dispersed and continuous phase and on the type of flow.

In inertia dominated break-up, which occurs when the drops are larger compared to the length scale of the Kolmogorov eddies, the droplets are broken up by pressure fluctuations. This force is of the order of ρU^2, where U equals the velocity fluctuation caused by the eddy. Also in this case the internal forces will try to maintain a spherical shape of the droplet. The ratio between this two forces is the ordinary Weber number, eq 4.

$$We = \rho U^2 R/\sigma \tag{4}$$

In analogy with the capillary number also for this Weber number the droplets will break-up when exceeding a critical value. It can be seen in eq 3 and eq 4 that both the dimensionless numbers are proportional to the droplet radius; this means that smaller droplets will not break-up as easy as larger droplets.

The stability of an emulsion refers to its ability to resist change in its properties over time. Break-down of emulsion can occur by various mechanisms [7]. As a result of the difference in density between the phases the droplets will either end up in the top or the bottom of the container, this is called creaming or sedimentation respectively. The droplets can also enter an energetically stable situation where the droplets are close to each other but still retain their integrity, this is called flocculation. These three mechanisms are reversible phenomena and the original state can often be regained. There are also more severe phenomena which are irreversible. These are coalescence where droplets merge into each other and Ostwald ripening where small drops lose material and finally disappear while larger drops grow in size. The later process is caused by diffusion of molecules of the dispersed phase through the continuous medium. To extend the lifetime of the emulsion, an emulsifying agent that stabilizes the emulsion can be added. An emulsifier stabilizes the emulsion by lowering the interfacial tension between the dispersed phase and the continuous phase.

There are several different methods for creating an emulsion. The three methods that are relevant for this project will be discussed in further detail below.

Stirring

Vessels with an agitator are the most commonly used type of equipment for blending liquids. Stirring of immiscible liquids is used to produce emulsions where the size of the dispersed drops will be determined by the balance between breakup and coalescence [6]. To change the balance to the favour of the breakup an emulsifier can be used.

The most typical arrangement of a baffled vessel with agitator, and the flow pattern generated, is shown in figure 3 from [8]. The mixing in the vessels can be either axial or radial depending on the type of impeller used. An impeller with tilted blades produces an axial flow while an impeller with flat blades produces mainly

radial flow. To prevent formation of a vortex, four vertical baffles are normally installed. These generate top-to-bottom mixing and improve effective mixing [9].

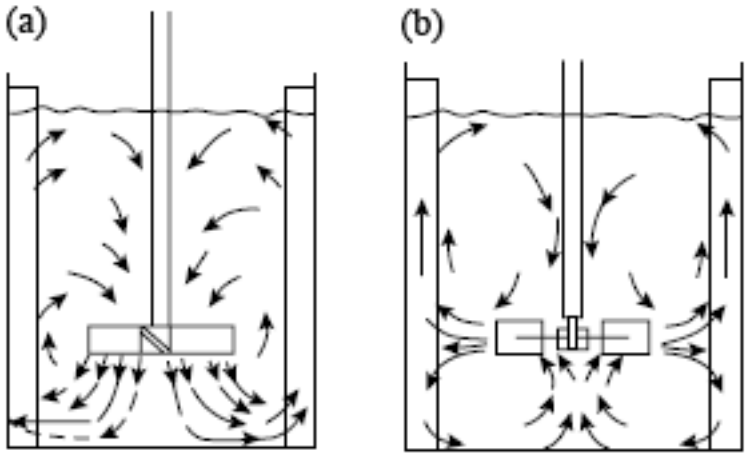

Figure 3: Typical arrangement of a baffled vessel with agitator. in (a) an impeller with tilted blades producing an axial flow and in (b) an impeller with flat blades producing a mainly radial flow [8].

In a stirred vessel there will be different types of flow; turbulent flow, with a chaotic nature, near the impeller and laminar flow at some distance from the impeller. A transition region with a flow somewhere between turbulent and laminar will also occur. Generally the type of flow occurring in a certain situation can be derived from the Reynolds number. For a stirred vessel the impeller Reynolds number can be used, eq 5, [9]. The length and velocity scales are based on the impeller diameter and tip speed.

$$Re_{imp} = ND_{imp}^2\rho/\eta \tag{5}$$

N is the rotational speed of the impeller (rev/s), D_{imp} is the diameter of the impeller and ρ and η are the density and viscosity for the liquid respectively. Different types and sizes of reactors require different impeller Reynolds numbers for turbulent flow. For example, the flow is turbulent in the whole vessel when the impeller Reynolds number exceeds 10 000 for a baffled vessel, the diameter of which equals the height of the emulsion volume and with an impeller diameter equal to one-half or one-third of the diameter of the vessel. The flow will be transitional for Reynolds numbers between 10 and 10 000, while the flow will be laminar for Reynolds numbers below about 10 [6]. Strong turbulent eddies leads to a larger Weber number and hence smaller droplets.

Static mixer

A static mixer, also known as motionless mixer, is standard equipment in the process industries for mixing fluids. It can be used for mixing two immiscible liquids and produce an emulsion. The prototypical design of a static mixer is a series of identical

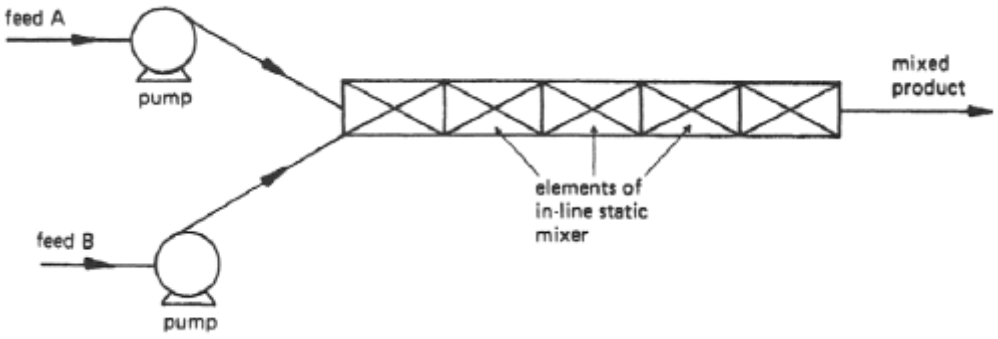

Figure 4: A schematic figure of a static mixer set-up [10].

motionless mixing elements installed in a pipe, see figure 3. The elements redistribute the fluid in the direction transverse to the main flow [10].

Similar to the emulsification process in a stirred vessel it is the shear stress in the turbulent flow that causes droplet break-up. As can be seen in eq 6, which shows the Reynolds number in pipes, a higher fluid velocity (V) through the mixer will give a higher Reynolds number. This in turn will give a higher Weber number, due to increased turbulence, which will result in smaller droplets [11].

$$Re = \frac{\rho V D_H}{\mu} \tag{6}$$

The advantages with a static mixer is its application for continuous emulsification process and the possibility to get a more even drop size distribution [11].

Membrane emulsification

Membrane emulsification is an emulsification technique where the dispersed phase is pressed through the pores of a membrane into the continuous phase. The continuous phase flows along the membrane surface at which the droplets grow in the pore openings until they have reached a certain size and detach. Surfactant molecules in the continuous phase stabilize the newly formed liquid-liquid interface to prevent droplet coalescence immediately after formation [12]. Contrary to the stirring and static mixer techniques, this technique is not dependent on turbulent mixing. Instead, the choice of membrane controls the droplet size. A narrower droplet-size distribution can be expected using this technique [13]. According to Joclyn and Trägårdh [13] who have published a couple of investigations about membrane emulsification, the typical membrane pore sizes range from about 0.05-14 µm. Commonly used membranes are tubular micro-porous glass (MPG) membranes and Shirasu porous glass (SPG) membranes. These membranes have cylindrical, interconnected, uniform micropores. They also state that it has been observed that the droplet size (d_d) of an emulsion have a linear correlation to the pore size (d_p) of the membrane, eq 7 with a constant x that typically ranges from 2-10.

$$d_d = x d_p \tag{7}$$

A typical experimental setup for membrane emulsification is described in several articles [12, 13, 14, 15]. The set-up incorporates a tubular membrane, a pump, a feed vessel and a pressurized container for the dispersed phase. Figure 5 from [13] shows a schematic picture of the setup. In this system the dispersed phase is pumped under gas pressure through the pores of the membrane into the continuous phase which circulates through the membrane module.

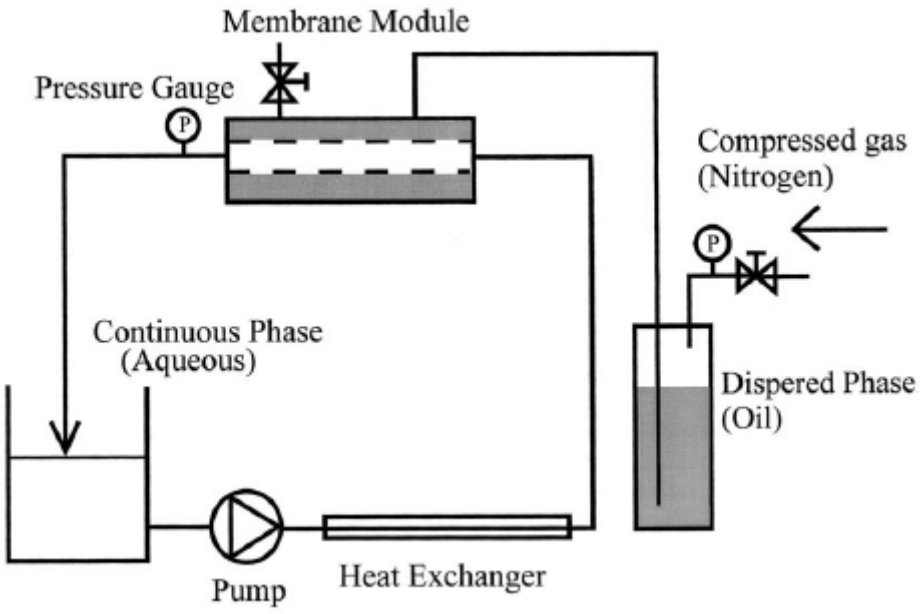

Figure 5: A schematic figure of a typical experimental setup for membrane emulsification [13]

.

2.3 Physico-chemical properties

2.3.1 Particle size

Silica gel particles have a size ranging from 1 to 100 µm and are always produced with a particle size distribution. The average particle diameter is usually specified with either a mean or a median value. The mean particle diameter can be defined as the mean diameter in number, d_n and the mean diameter in surface, d_s, or the mean diameter in volume (or mass), d_v, as in equation 8, 9 and 10.

$$d_n = \sum n_i d_i / \sum n_i \tag{8}$$

$$d_s = \sum n_i d_i^3 / \sum n_i d_i^2 \tag{9}$$

$$d_v = \sum n_i d_i^4 / \sum n_i d_i^3 \tag{10}$$

Where n_i is the number of particles with diameter d_i [1].

The median divides the distribution into two equal parts, it is the 50% size on the cumulative distribution curve, and are usually denoted d_{v50}. On the cumulative

distribution curve, the diameter at 10% and 90% are also of interest, they are used to calculate a $d_{v90/10}$ value that gives an indication of the distribution of the particle size.

Particle size determination

There are several techniques available to determine the particle size of a sample. Microscopy is the simplest method but it is only useful for rough estimations. In this project, two other methods for particle size analysis have been used; flow particle image analysis (FPIA) and electrical sensing zone (ESZ) also named the Culter method.

Image analysis with microscope is a time consuming method, FPIA is an automated image analysis technique that can count up to several hundred thousands of particles in a short space of time. A sample from a dilute suspension of particles is passed through a measurement cell where images of the particles are captured. The instrument used in this project is a FPIA 3000 from Sysmex/Malvern. The FPIA 3000 uses a CCD-camera that captures the particles as they pass through the cell. The instrument captures images in real time and analyzes them in terms of their morphological parameters to produce corresponding size and shape distributions.

The ESZ technique is described by Xu in [16]. In ESZ, the particles are dispersed in an electrolyte and forced through a small aperture. The aperture is placed between two electrodes with a constant electric current over. When a particle passes through the aperture, it displaces its own volume of conducting liquid, momentarily increasing the impedance of the aperture giving rise to a voltage pulse. The amplitude of the pulse is proportional to the particle volume and the number of pulses is the number of particles measured. For each instrument a calibration constant, K_d, is used to translate the voltage readings to particle diameter. The particle diameters of porous particles will be under-estimated due to inclusion of an electrolyte which lowers the impedance. The change in the impedance of the aperture will hence be smaller compared to a solid particle with an equivalent particle diameter. To compensate for the porosity of the silica particles, mass calibration should be used.

2.3.2 Specific surface area

The specific surface area of a porous solid is equal to the sum of its internal and external surface areas and are given in m^2/g [2]. The specific surface area of silica gels used in high-performance liquid chromatography ranges from 10 to about 500 m^2/g [1]. Surface area is routinely measured using the BET method described below.

In the BET-method, data from a gas adsorption isotherm are put into the BET-equation, which is used to calculate the specific surface area. The BET-equation is named after the inventors Brunauer, Emmett and Teller. Gas adsorption isotherms are determined at different relative pressures at a temperature at which the gas is in the liquid state (77 K for nitrogen). Within the isotherm equations there exist parameters which are associated with surface area. To extract these parameters a least-squares routine is used to determine the surface area. The fit for the BET isotherm is valid only over a certain linear range of the curve.

The original form for the BET equation, eq 11

$$\frac{V}{V_{mon}} = \frac{Cx}{(1-x)(1+(C-1)x)} \qquad \text{where} \qquad x = \frac{P}{P_s} \tag{11}$$

where V indicates the volume of gas adsorbed at STP (standard temperature and pressure), V_{mon} is the volume of gas required for a monolayer, P_s is the vapour pressure of the bulk liquid at the same temperature, P is the adsorptive pressure and C is a constant.

For analysis, the equation rearranges into the transformed form, eq 12 to give a linear relationship. For the analysis made in this project the linear range used is between 0-0.25 P/P_s

$$\frac{x}{V(1-x)} = \frac{1}{CV_{mon}} + \frac{C-1}{CV_{mon}}x \tag{12}$$

Using the the slope S_{BET} and the intersect I_{BET}, the monolayer volume V_{mon} can be determined.

$$V_{mon} = \frac{1}{S_{BET} + I_{BET}} \tag{13}$$

From V_{mon} one can obtain

$$C = \frac{1}{V_{mon} I_{BET}} \tag{14}$$

For BET, V_{mon} can be related to the number of gas atoms in a monolayer, eq 15.

$$n_m = \frac{V_{mon}}{22400} \tag{15}$$

In the case of N_2 adsorption IUPAC has set a conversion factor to convert V_{mon} into a surface area number, the IUPAC convention settled on 16.2 Å^2 (0.162 nm^2) per nitrogen molecule as a standard [17], denoted a in forthcoming eq 16.

$$A_s = \frac{n_m a}{m} N_A \tag{16}$$

Where m is the samlpe mass in grams.

2.3.3 Porosity

Pores can be defined as holes, cavities or channels communicating with the surface of the solid. A cavity that does not communicate with the surface is called a closed pore or an internal void and will not contribute to the porosity or specific surface area.

Pores can have many different shapes and the width of the pore is defined as, p_d, which is the diameter of an equivalent cylindrical pore. The classification of pores according to IUPAC, is micropores with $p_d < 2$ nm, mesopores with $2 < p_d < 50$ nm and macropores with $p_d > 50$ nm.

The porosity of a sample is defined as the total pore volume, V_p, divided by the total volume of the sample, V_T. The total volume of the sample is the sum of the pore volume and the volume of solid silica, assuming there are no closed pores. The pore volume and pore size distribution can be estimated using gas adsorption-desorption isotherms.

According to Sing [17] the adsorption isotherms of gas onto solids can be arranged in six different types, figure 6. Type I, IV and V isotherms show hysteresis, i.e., the desorption branch of the curve does not coincide with the adsorption branch. The hysteresis is used for determination of pore size distribution and pore geometry. The three isotherm types correspond to microporous, mesoporous and polydisperse porosity respectively. The BET isotherm is a type IV isotherm and can hence be used for determination of pore volume of mesoporous silica particles. Nitrogen, at the nitrogen boiling point (77 K), is the most commonly used gas for sorption studies. The gas sorption method produces accurate results in the pore size range between 0.5 and 50 nm [1].

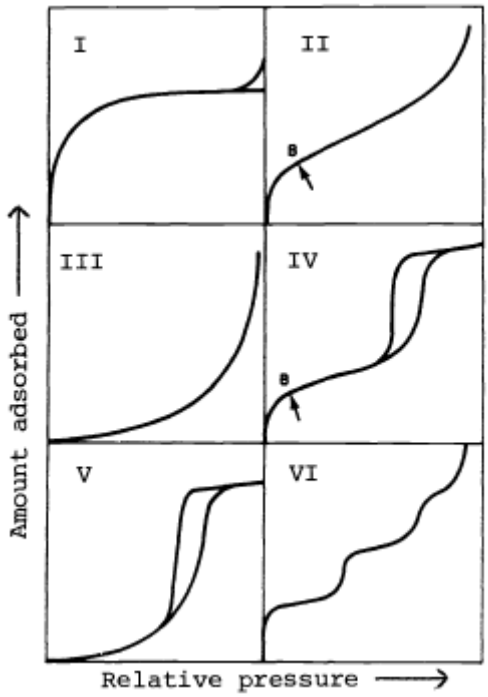

Figure 6: Six different types of gas adsorption isotherms [17]

.

Further information about pore volume determination is considered to be outside of the scope of this report.

3 Experimental method

This chapter summarizes the materials and the methods used. Experimental set-ups, theory behind the experiments and the procedures in short are described.

For all gelling experiments, reactors with the possibility to control temperature, pressure and stirring speed have been used. A schematic picture of the gelling reactor set-up used in all experiments is shown in figure 7. Two different reactors have been used; a lab scale reactor and a pilot scale reactor.

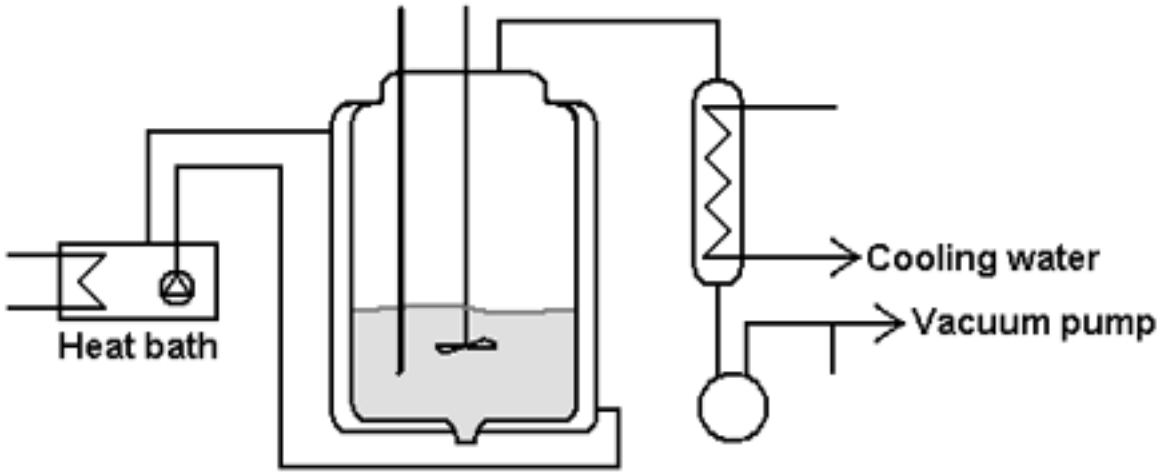

Figure 7: A schematic picture of the gelling reactor setup used in all experiments.

Lab scale reactor

The lab scale reactor is a glass reactor with a volume of 10 litres. It is heated with water in a surrounding jacket on the whole lateral area and bottom. The impeller has two blades which both are pitched twice, see figure 8. In the reactor there are one baffle and one cylindrical glass rod containing a thermometer.

Figure 8: The impeller blade geometry of the impeller in the lab scale reactor.

Pilot scale reactor

The pilot scale reactor, volume 200 litres, is made of stainless steel and heated over either the whole or half of the lateral area with oil. It has a four bladed stirrer with pitched blade impeller geometry, see figure 9, and four baffles.

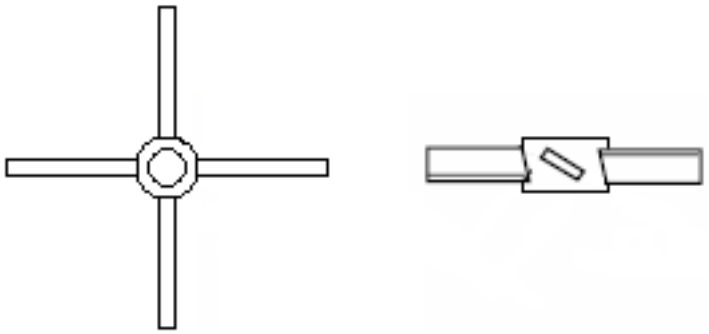

Figure 9: The impeller blade geometry of the impeller in the pilot scale reactor.

For all gelling processes, the temperatures and pressures were monitored in iFIX, charts are available in appendix B.

All experiments were performed in a similar way. The procedure can be divided in five main parts; emulsification, gelling, washing, calcination and rehydroxylation. For the gelling step, two different approaches have been used. In the experiments where the size is of interest, a salt has been added to start the gelling process at high temperature, while in the experiments where the surface area is of interest, the gelling has been done by evaporation of water at a lower temperature and reduced pressure. The filtration and washing steps were performed in filter funnels with an integrated sintered glass filter disc of porosity four if nothing else is specified.

3.1 Membrane emulsification

These experiments aim to investigate if a plastic wire mesh can be used as a simple membrane to control the particle size and get a narrow particle size distribution.

Experiments with three different mesh sizes and a reference experiment without wire were performed in the lab scale reactor. One scale up experiment was performed in the pilot scale reactor.

3.1.1 Set-up

The set-up consisted of a plastic pipe with a wire covering the bottom opening, see figure 10 a, through which the silica sol was added to the continuous phase. The wire was a plastic mesh normally used in paper making. The meshes had a quadratic geometry as can be seen in the photography of the 125 µm in figure 10 b.

A sketch of the principal theory of the emulsification in these experiments is shown in figure 11.

3.1.2 Experimental procedure

To make an emulsion, silica sol was added to the continuous phase, containing an emulsifying agent, through the plastic pipe with different wires. The meshed pipe opening was held approximately at the same height as the impeller blade and in

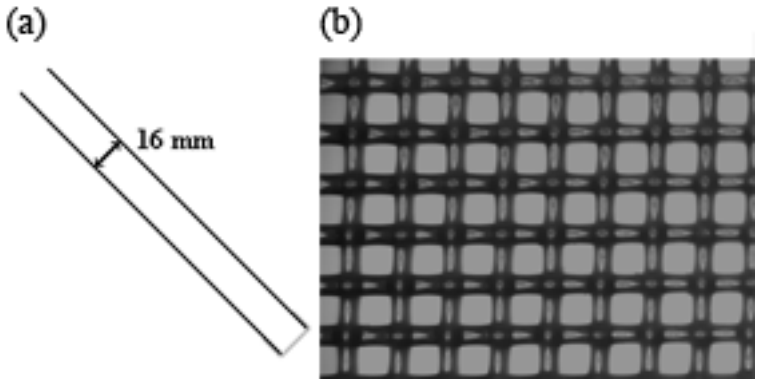

Figure 10: In (a) a plastic pipe with wire used for the membrane emulsification experiments and in (b) a photography of the 125 µm wire mesh.

the middle between the tip of the impeller blade and the reactor wall during the addition of the sol. The continuous phase was under stirring during the adding of the sol, for which the flow rate was about 625 g per minute. To initiate the gelling process of the silica, the emulsion was heated to 80 ℃ and a salt was added. The emulsion was kept at 80 ℃ during one hour, after which water was evaporated by stepwise reduction of the pressure in the reactor while keeping the temperature of the heat bath constant at 80 ℃. The formed gel particles were filtered and washed with ethanol before they were dried in an oven at 90 ℃. The dry gel was calcinated in an oven at 630 ℃ for five hours. Finally, a rehydroxylation step was performed where the gel was heated in ammonia for two hours, acidified by addition of nitric acid, filtered and washed with water and acetone.

In the first experiment, ME 1, a wire with mesh size 71 µm was used. The stirring speed was 400 rpm during the emulsification and 300 rpm during the first part of the gelling. After a few hours a white gel layer was visible at the bottom of the reactor. In an attempt to resuspend the gel layer, the stirring speed was increased to 500 rpm. This had little effect on the gel layer in the bottom and in a second attempt to resuspend the layer the vacuum in the rector was released and the layer was scraped off with a plastic rod. The experiment then proceeded as described above.

During the second experiment, ME 2, wire mesh size 125 µm, the stirrer was lowered a few centimeters to investigate if the gel layer in the bottom of the reactor could be avoided. The stirring speed was 400 rpm during the emulsification and gelling. This had very little effect on the layer in the bottom and the layer was again resuspended by scraping with a plastic rod.

The stirring speed seemed to have little or no effect on the formation of a layer in the bottom of the reactor and all experiments after were performed with a stirring speed of 300 rpm during the emulsification and gelling.

In the third experiment, ME 3, wire mesh size 71 µm, the gel layer in the bottom of the reactor was left in the reactor and discarded.

After these attempts to avoid the formation of a gel layer in the bottom of the reactor a series of experiments, ME 4-ME 7, with three different mesh sizes and a reference experiment without wire was then performed. 300 rpm stirring was used through the whole series and mesh sizes used were 20 µm, 71 µm and 125 µm. The

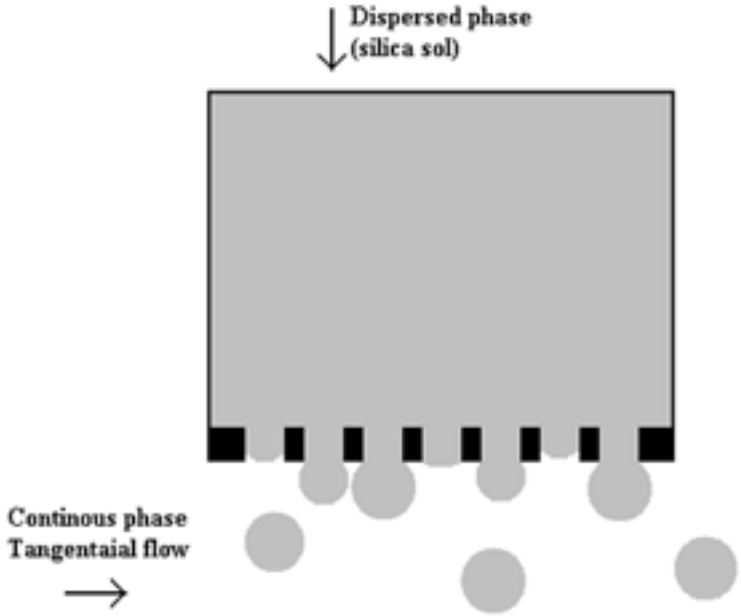

Figure 11: The dispersed phase is pressed through the membrane into the continuous phase.

gel layer in the bottom was resuspended after the emptying of the reactor and pooled with the rest of the gel during the washing rehydroxylation step.

One scale-up experiment, ME 8, was performed in the pilot scale reactor. The stirring speed was 60 rpm which corresponds to 300 rpm in the lab scale reactor. No gel layer was formed in the bottom of the reactor. The gel was filtered and washed in a centrifuge. The calcination was performed in the same way as the lab scale experiments but the rehydroxylation was performed in a 25 litres glass reactor. The washing part of the rehydroxylation was performed in nine consecutive filtration runs during two days in a filter funnel. The unwashed gel was stored in the acidic solution from the rehydroxylation.

An overview of the experiments is shown in table 1.

Table 1: The membrane emulsification experiments.

Experiment	Mesh size (µm)	Stirring speed (rpm)
ME 1	71	400/300/500
ME 2	125	400
ME 3	71	300
ME 4	20	300
ME 5	71	300
ME 6	125	300
ME 7	none	300
ME 8 - pilot scale	125	60

3.2 Emulsification with static mixer

The aim of these experiments was to produce small particles around 2 µm with a narrow particle size distribution.

3.2.1 Set up

The static mixer setup consisted of two peristaltic pumps with analog speed controllers and a plastic pipe containing static mixer elements. For the continuous phase, a Masterflex model 7554-20, 6-600 rpm with easy-load pump head model 7518-00 and a Masterflex Tygon Lab tubing model 6409-17 were used. For the sol phase, Masterflex model 7553-85, 1-100 rpm with quick-load pump head model 7021-20 and a Masterflex Norprene tubing model 6404-16 were used. Calibration curves for the pumps are available in appendix A. A reducer with a diameter of 1.5 or 2 mm was placed downstream 10 mixing elements inside a plastic pipe. For a schematic picture of the set-up see figure 12.

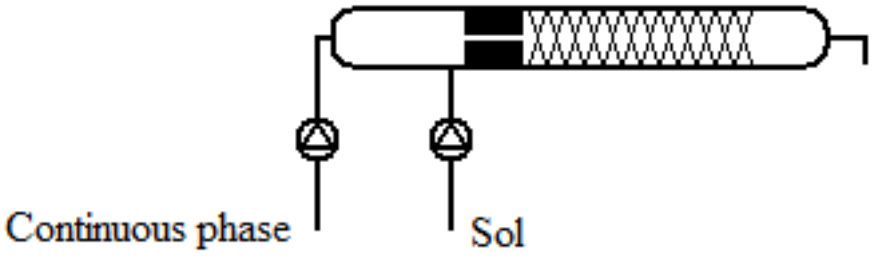

Figure 12: A schematic picture of the static mixer emulsification set-up.

Three different reducers with an inner diameter of 3 mm, 2 mm and 1.5 mm were produced. Only the two smallest were used in the gelling experiments.

3.2.2 Experimental procedure

An emulsion with silica sol as the dispersed phase was produced with a static mixer. Three experiments were performed, SM 1 - SM 3, with different flows and different reducers, see table 2. The emulsion was collected and transferred to the lab scale gelling reactor. The gelling procedure in the reactor followed the same procedure as for the membrane emulsification; the emulsion was heated to 80 ℃, addition of a salt and evaporation of water by stepwise lowering of the pressure during which the stirring speed was 400 rpm. The gel was washed with ethanol, calcined at 630 ℃ and rehydroxylated with ammonia in the same way as described for the membrane emulsifications experiments.

The ratio by weight of sol to continuous phase with emulsifying agent was approximately 6.8. The flow rates of the pumps were hard to control due to the analog speed controllers. For all three experiments the flow rate is a rough approximation.

Table 2: The static mixer emulsification experiments.

Experiment	Reducer diameter (mm)	Flow rate (ml/min)	Velocity in reducer (m/s)
SM 1	1.5	160	1.5
SM 2	2.0	770	4.1
SM 3	1.5	850	8.0

3.3 Stirring emulsification

This type of experiment, ST 1, was only performed in the pilot scale reactor. According to theory, a higher stirring speed will lead to smaller particles.

3.3.1 Experimental procedure

The sol was added to the continuous phase through a metal pipe, permanently installed under the surface close to the wall of the reactor, with a velocity of about 0.8 litres per minute. The stirring speed was 180 rpm. The emulsion was left to emulsify for one hour before raising the temperature. The gelling was executed with the same gelling procedures as described in more detail in the membrane emulsification experimental procedure part; heating of the emulsion to 80 ℃, addition of a salt and evaporation of water by stepwise lowering of the pressure. During the evaporation the stirring speed was set to 60 rpm. After the evaporation, the vacuum was released and the gel was left in the reactor over night. The gel was then filtered and washed with acetone and ethanol in a centrifuge and was calcined at 630 ℃ in five hours. The rehydroxylation was performed in a 25 litres glass reactor with ammonia. The washing part of the rehydroxylation was performed in nine consecutive filtration runs during five days in a filter funnel. The unwashed gel was stored in the acidic solution from the rehydroxylation.

3.4 High surface sols

In the experiments presented in this section, one acidic sol and two sols stabilised with different amount of NaOH have been gelled. Since the surface of the sols decrease with increased temperature, the evaporation temperature was kept low.

3.4.1 Set-up

The lab scale reactor was used for all high surface sol experiments. A plastic tube was used for adding the sol to the continuous phase.

3.4.2 Experimental procedure

The sol was added to the continuous phase trough a plastic tube approximately 2 cm under the surface, 625 grams during one minute. The stirring speed was 400 rpm during the emulsification and 300 rpm during the gelling. The gelling procedure was different from the previously described experiments. The temperature of the

water bath was set to 80 ℃ and the pressure in the reactor was set to 90 mbar. Evaporation of water started when the reactor temperature was around 50 ℃ and continued until it had reached 80 ℃. The gel was filtered, washed with ethanol and dried at 90 ℃. Before the calcination, the gel was refluxed in acid, 1.5% HNO_3 (aq), for several hours. The gel was calcinated and the surface area and porosity were measured.

The three first experiments, HS 1 - HS 3, were performed with a water glass containing 5% SiO_2 as starting material. The water glass was stabilised with NaOH to SiO_2:Na_2O molar ratios of 20:1 and 10:1. The sol with molar ratio 20 was used for one experiment and the sol with ratio 10 was used for two experiments, one with the initial SiO_2 concentration and one that was concentrated by ultra filtration.

The gelling experiments were performed in the following order: first the sol with molar ratio 20, then molar ratio 10 with the initial SiO_2 concentration and last molar ratio 10 concentrated. The sols were stored at 4 ℃until the gelling and one experiment was performed every day.

A water glass containing 4.8% SiO_2 and a SiO_2.Na_2O molar ratio of 3.3:1 was produced by heating a fumed SiO_2 powder in NaOH (aq) for three hours. The water glass was then ion exchanged to exchange sodium ions for hydrogen ions. The formed sol, HS 4, was emulsified, gelled, acid boiled and calcinated under the same conditions as the Na-stabilised sols.

4 Results

The results will be presented in three subsections according to their purpose. All FPIA 3000 analysis reports are available in appendix C.

4.1 Large silica gel particles

The particle sizes were measured only with the FPIA 3000. Size measurement results for the three initial experiments are presented in table 3. Neither different mesh sizes, stirring speeds nor the placement of the stirrer had any significant effect on formation of a gel layer at the bottom of the reactor.

Table 3: Results for the membrane emulsification experiments.

Sample	Mesh size (µm)	Mean diameter d_v(µm)	Median diameter d_{v50}(µm)	Size distribution $d_{v90/10}$
ME 1	71	22.5	22.5	2.6
ME 2	125	39.5	37.6	2.7
ME 3	71	36.7	37.6	2.8

The results for the series of experiments, ME 4 - ME 7, made under the same stirring conditions are presented in table 4 and the mean particle diameter as a function of the mesh size is shown in figure 13.

Table 4: Results for the membrane emulsification experiments.

Sample	Mesh size (µm)	Mean diameter d_v(µm)	Median diameter d_{v50}(µm)	Size distribution $d_{v90/10}$
ME 4	20	43.8	43.7	2.5
ME 5	71	41.0	41.7	3.6
ME 6	125	48.9	49.9	2.6
ME 7	reference	38.1	37.0	2.4

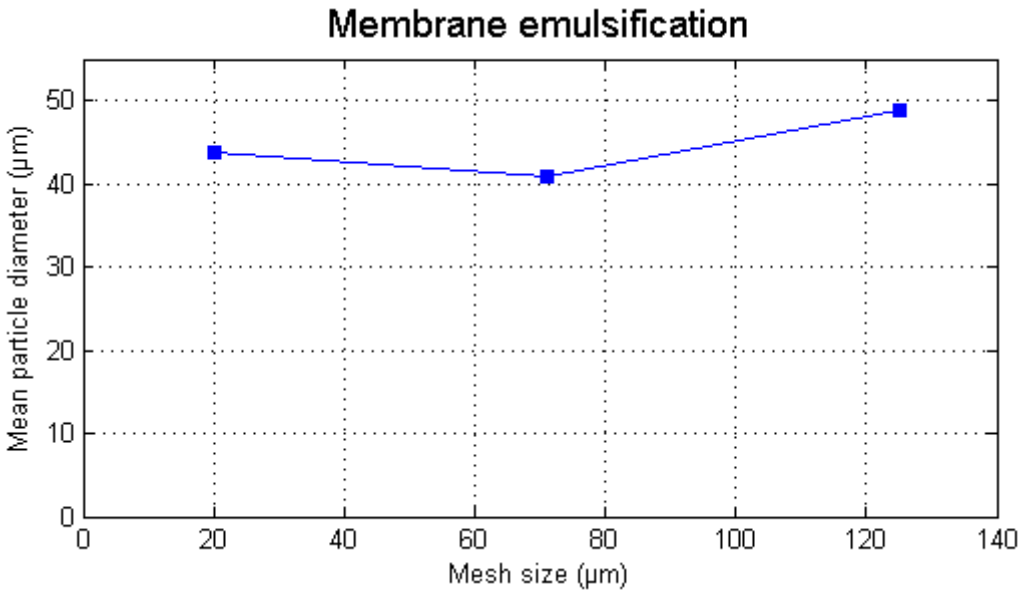

Figure 13: Results for the membrane emulsification experiments.

Pictures of all samples made were taken in a light microscope. Pictures of the samples from the experimental series ME 4 - ME 7 are shown in figure 14. It is more flakes in the reference sample, ME 7.

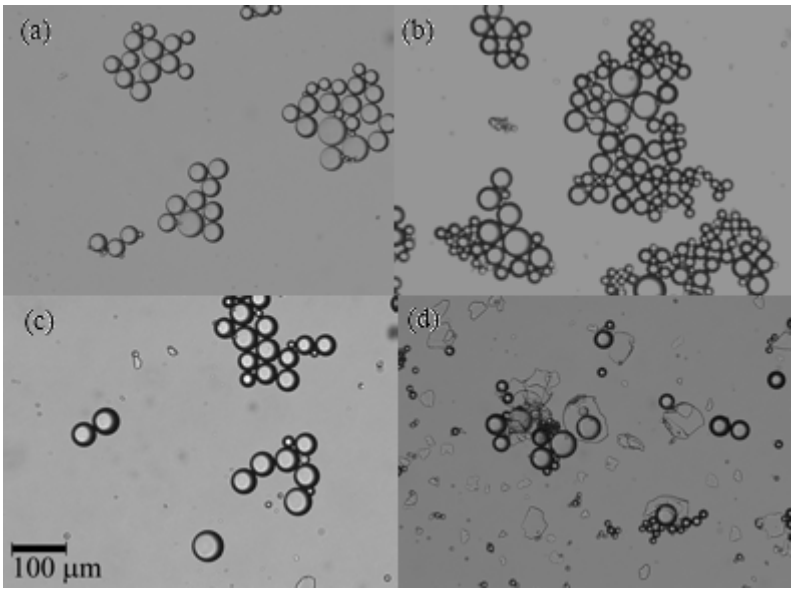

Figure 14: Pictures of the samples from the experimental series, (a) ME 4, (b) ME 5, (c) ME6 and (d) ME 7.

Particles from the pilot scale experiment, ME 8, were measured with FPIA 3000 and specific surface area and specific pore volume were measured with the N_2 adsorption desorption method. The mean diameter was 41.4 µm, the d_{v50} was 37.4 µm

and the $d_{v90/10}$ was 2.8. The BET area was 343.0 m^2/g and the specific pore volume was 1.2 cm^3/g.

Pictures of the samples have been taken both with light microscopy and SEM, see figure 15.

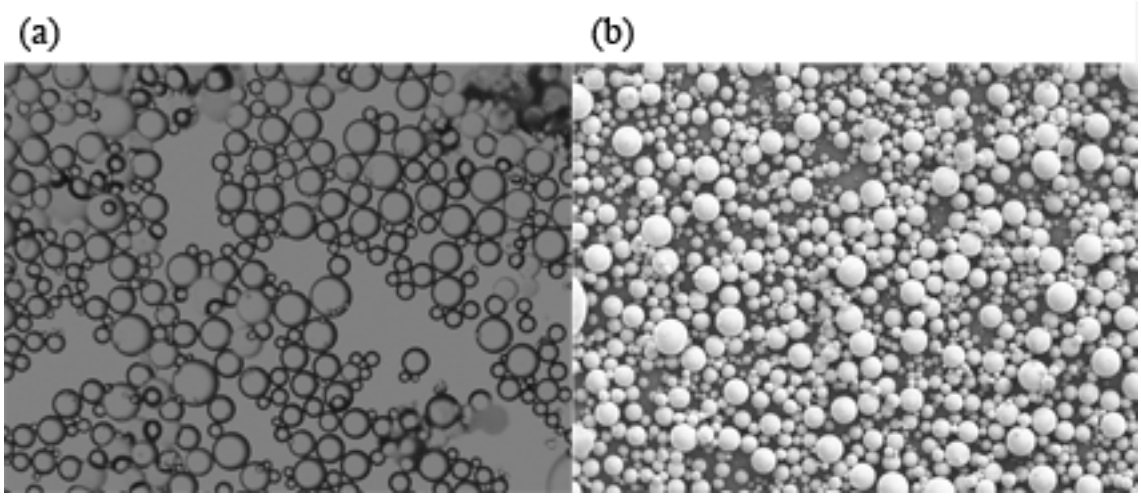

Figure 15: Pictures of ME 8, (a) have been taken in light microscopy and (b) with SEM.

.

4.2 Small silica gel particles

4.2.1 Static mixer

Particle size measured with FPIA 3000 are presented in table 5, and the particle size as a function of the mean velocity in the reducer is shown in figure 16.

Table 5: Results for the static mixer emulsification experiments.

Sample	Velocity in reducer (m/s)	Mean diameter d_v (μm)	Median diameter d_{v50} (μm)	Size distribution $d_{v90/10}$
SM1	1.5	29.1	28.9	3.4
SM2	4.1	16.2	15.4	4.7
SM3	8.0	8.3	6.2	4.8

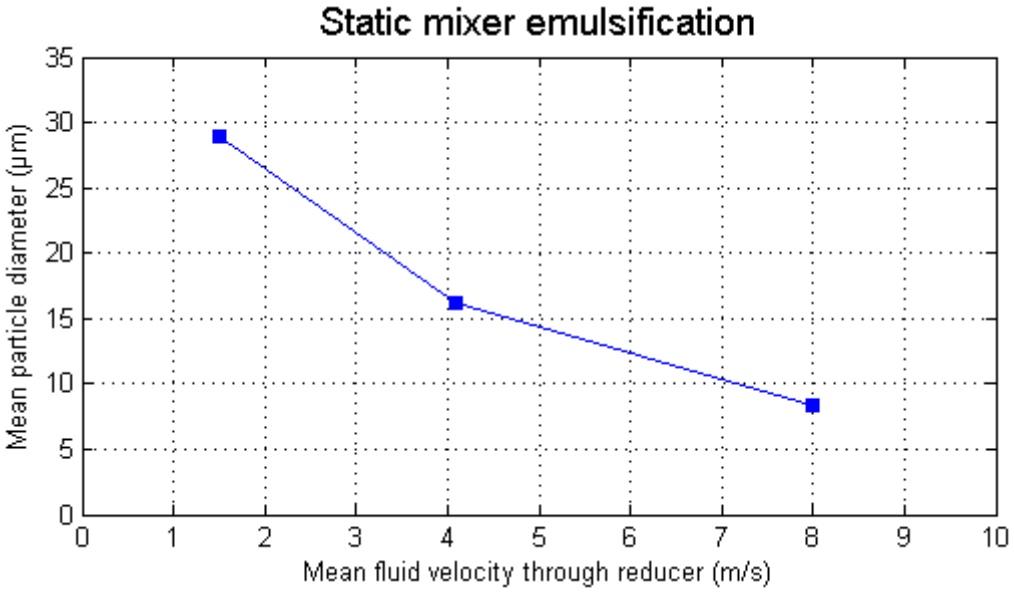

Figure 16: The particle size as a function of the mean velocity in the reducer of the static mixer set-up.

Pictures of the samples from the experimental series is shown in figure 17.

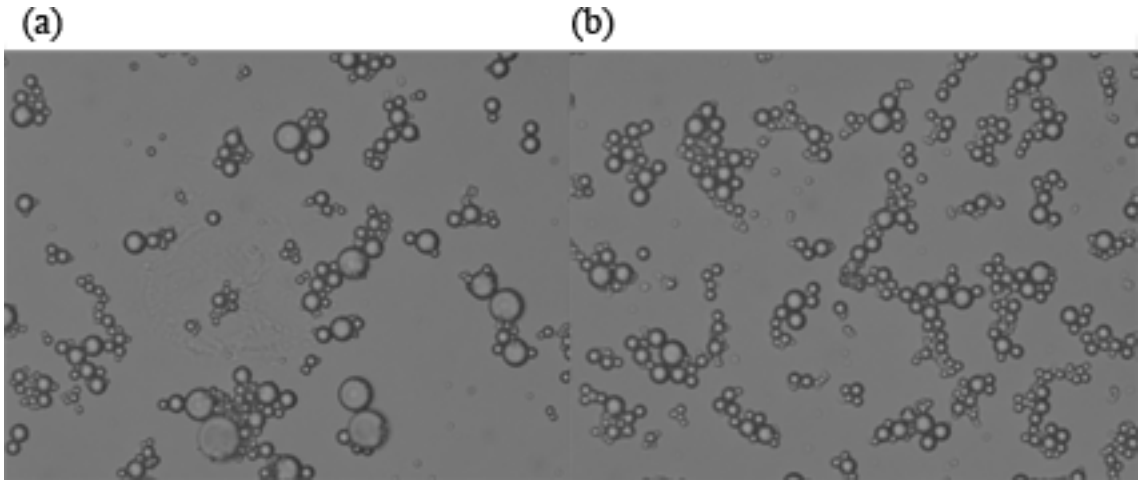

Figure 17: Pictures showing particles from the static mixing emulsification experiments. In (a) SM 2 and in (b) SM 3.

4.2.2 Stirring

The particle size analysis from the pilot scale experiment with high stirring speed were made both with a FPIA 3000 and with a Beckman Coulter counter.

When using the FPIA to analyse the sample the mean diameter was 3.8 µm, the median diameter was 3.5 µm and the $d_{v90/10}$ was 3.3. The corresponding results when using the Beckman Coulter counter were a slightly higher median diameter

of 3.6 µm and a $d_{v90/10}$ of 3.8. For this sample, the specific surface area was 337.4 m^2/g.

4.3 High surface area particles

Results from measurements with N_2 adsorption desorption technique are presented in the following sections.

4.3.1 Sodium stabilised sol

Results from specific surface area, pore diameter and pore volume measurements are presented in table 6.

Table 6: Results for the high surface area experiments.

Sample	SiO_2:Na_2O	Storing time (days)	BET surface (m^2/g)	Pore volume (cm^3/g)	Pore diameter (Å)
HS 1	20	0	261.7	1.23	188.5
HS 2	10	3	139.4	0.57	164.7
HS 3	10	4	105.5	0.77	291.9

The sols were stored for some days before the gelling experiment were performed, figure 18 shows the measured BET surface area as a function of storing time.

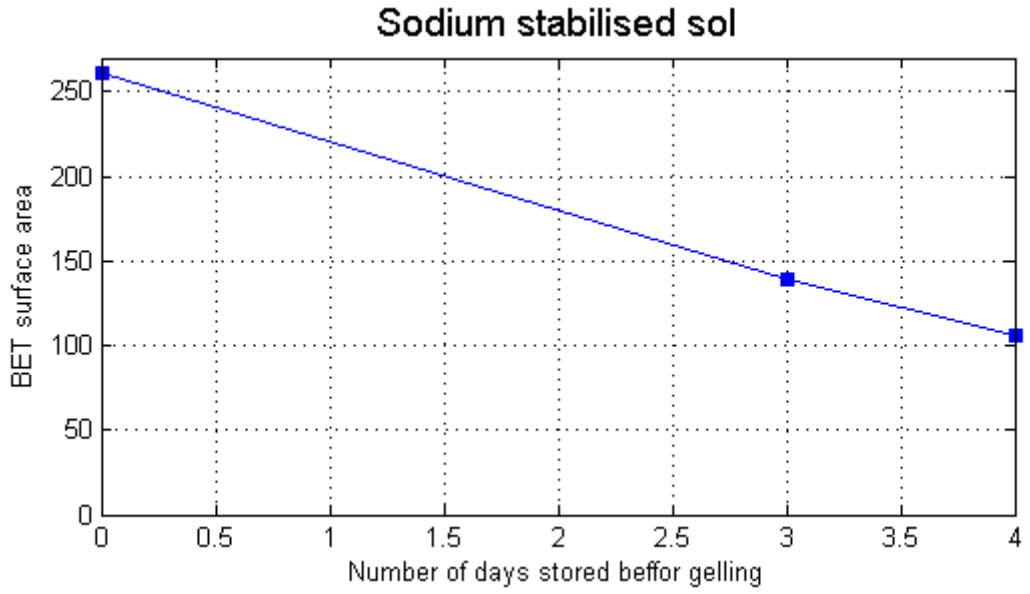

Figure 18: The BET surface area as a function of storing time.

4.3.2 Acidic sol

The gel produced from the acidic sol, HS 4, had a BET area of 439.3 m^2/g, a pore volume of 1.66 cm^3/g and a pore diameter of 145.6 Å.

5 Discussion

In this section the results and methods are discussed. A gel made by Separation Products is shown as a reference sample, see figure 19. The gel was made by adding the silica sol at a stirring speed of 400 rpm and then gelling the emulsion without salt addition. The sol was added through a plastic tube. The particle size was measured by Coulter counter and the median diameter was 10.8 µm and the $d_{v90/10}$ was 3.0.

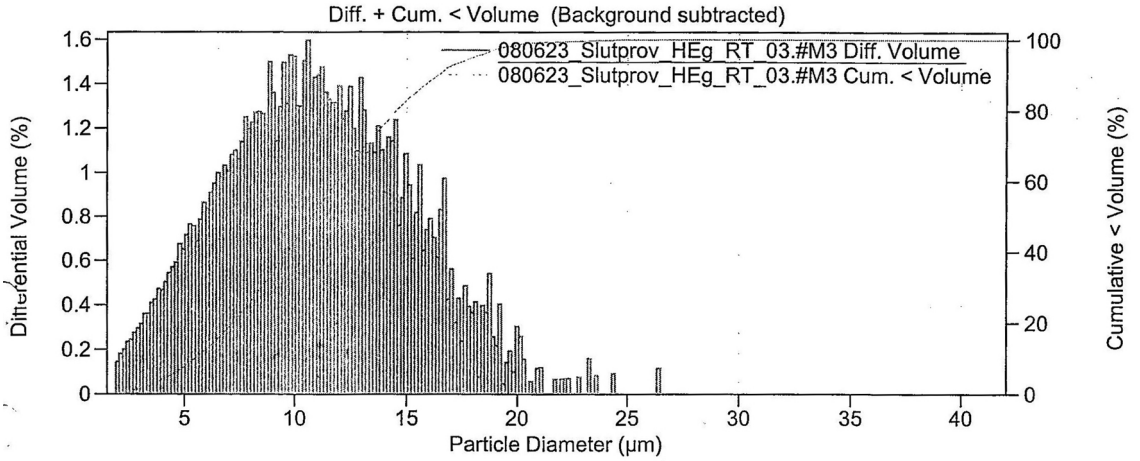

Figure 19: The Coulter counter result for a a reference gel made by Separation Products.

5.1 Large silica gel particles

The aim was to produce larger particles with narrower particle size distribution in order to get a higher yield of larger particles from a batch. The produced particles in the pilot scale experiments were definitely larger with a median diameter of 37.4 compared to the reference batch witch have a median diameter of 10.8 and almost no particles larger than 19.5 (d_{v90}).

A problem with the gelling in the lab scale reactor was the formation of a gel layer in the bottom of the reactor. Due to the opacity of the emulsion it was hard to determine if the gel layer was formed at the gelling step or during the evaporation of the water. No solution to the problem was found but it does probably not affect the outcome of the experiment much since the result for the experiment where the gel layer was discarded did not differ much from the rest of the experiments. In the pilot scale reactor the problem with a gel layer on the bottom of the reactor was not present. The probable explanation to this is the different impeller geometry and size in relation to the diameter of the vessel which produces a much stronger axial flow, see figure 3. It was not possible to determine if the particles sedimented due to their larger size or if there were aggregates of particles and flakes that sedimented or attached to the glass wall of the reactor. A possible contributing factor could be that the particles might have a stronger affinity for the glass walls in the lab setup than for the stainless steel walls of the pilot scale reactor.

Whether the wires had any actual effect on the particle size and size distribution is hard to determine from the performed experiments. The result from the FPIA 3000 shows that there are almost no difference between the reference sample and the samples made using membrane emulsification. Microscopy showed clearly that the reference sample was full of flakes and had fewer spherical gel particles then the samples made with wire, which makes the result from these analyses contradictory and puts into question the reliability of the FPIA 3000. If the yield of large particles is of interest, the ability to measure the amount of flakes is of course important as well. The wire probably had a dampening effect on the velocity of the sol before it entered the agitated continuous phase which could be the reason why there are less flakes and more spherical particles in the samples made with wire.

Literature states that there is a linear relationship between particle size and membrane pore size [13]. This relationship has not been observed for the performed experiments. One reason for this could be the difference in setup compared to those found in literature. In the used setup, stirring as well as membrane is applied while the setups found in literature had no impeller present that could destroy the formed droplets. The setup used in this project could be expected to give a relationship that is a mixture of the one for stirring and the one for membrane emulsification because the stirring will be limiting to the maximum droplet size. This implies that particles with narrow particle size distribution could be produced as long as the droplets emerging from the membrane are not large enough to be destroyed by the impeller. Small particles produced with wire could hence show a narrow particle size distribution while a wire that causes large droplets to be formed would yield a broad size distribution after stirring.

Assuming that the particle size and distribution results obtained from analysing the reference sample is reliable, it can be concluded that the cause for larger particles being produced is not primarily the wire mesh but something else. The reference sample produced before the project started by Separation Products is made using a flexible plastic tube which has a smaller diameter and is slightly curved. When the sol is added, the velocity could be expected to be lower than for the stiff plastic tube almost perpendicular to the surface. The effect of stirring speed, as indicated by the results, seems to be significant but definitely not large enough to account for the total increase in particle size on its own. The final major difference in the procedures is how the gelling was performed. The reference sample is boiled before gelling which probably leads to droplet breakup with smaller particles as a result. It can be concluded that the addition of salt that causes gelling before evaporation of the dispersed phase leads to larger particle sizes.

To be able to draw any reliable conclusions from this work it is obvious that more experiments need to be made. First of all a more reliable reference sample without wire needs to be produced. Then different sol-addition flows should be tested, preferably with a pump where the flow rate can be constant and controlled. The glass reactor could use a better impeller which produces a stronger axial flow to perhaps reduce the impact of layer formation in the bottom. To make the experiments more reproducible and less time consuming for the operator an automated vacuum pump for pressure reduction in the reactor is preferred compared to manually adjusting the pressure during several hours when evaporating the dispersed phase.

5.2 Small silica gel particles

The limiting factors for the static mixer experiments were the pressure limit for the plastic tubes and pipes and the capacity of the peristaltic pumps. The result was promising and a distinct, almost linear, correlation between the velocity in the reducer and the particle size was obtained.

The particle size distribution was, however, not narrowed compared with when using the standard gelling method. It can be noted that the size distribution broadens slightly with increased velocity but it should also be noted that the FPIA 3000 is used also for this measurements and that the difference in distribution could be within its error margins. The way peristaltic pumps function could possibly also play a part in how the particle size distribution turns out. A peristaltic pump is a positive displacement pump which uses a rotor with a number of rollers. As the rotor turns, the part of the tube under compression closes thus forcing the fluid to be moved through the tube. This causes a pulsing flow and the velocity of the fluid varies with the pulses.

It was hard to regulate the flow from the pumps due to the analog speed control. To continue the work pumps with a constant non pulsing flow and digital speed controller to get an increased reproducibility of the experiments would definitely be preferable.

The pilot scale experiment stood on its own and was performed because the static mixer setup was insufficient for producing the desired yield of the sought particle size. The experiment was based on the fact that increased stirring leads to more droplet breakup and earlier experience from the supervisor of the project.

When it comes to the experimental part of the pilot scale experiment, it is to recommend that the filtration and washing after the rehydroxylation step is performed in a centrifuge, both to save time and to get a cleaner product. The filtration of small particles takes very long time in funnels since the filter cake gets very compact.

5.3 High surface area particles

The different grades of Kromasil particles produced at Separation Products, from silica sol, have the following relations between the pore size and the specific surface area: Samples with a pore diameter of 60 Å have a specific surface area of around 550 m^2/g, a diameter 100 Å gives 320 m^2/g and a diameter of 300 Å have a specific surface area of about 110 m^2/g.

The result showing the largest specific surface area for the sodium stabilised sol samples had an area of 291.9 m^2/g and a pore diameter of 105.5 Å. This indicates that this sample have a similar area to pore size ratio compared to the Kromasil particles described above.

The relatively low specific surface area of the sodium stabilised samples is probably due to the high pH of the sol which results in too large sol particles before gelling takes place. For a pH between 10 and 11 the solubility of silica in the sol is high and hence the particle growth is fast, see section 2.1. Because of the growth of the sol particles the specific surface area was lower for the samples that had been stored in the fridge. However the sols were stable and did not gel during this time.

The unstabilised sol gave gel particles with a pore diameter 145.6 Å and a specific surface are of 439.3 m^2/g. This surface are seem to be quite large in relation to the pore diameter if compared to for example the 100 Å Kromasil product that has a specific surface area of 320 m^2/g. A major drawback here is of course the instability of the sol which makes it difficult to handle due to its fast gelling rate.

To get an over wive of the different sols and the Kromasil reference material, the measured surface area as a function of the pore diameter is shown in figure 20.

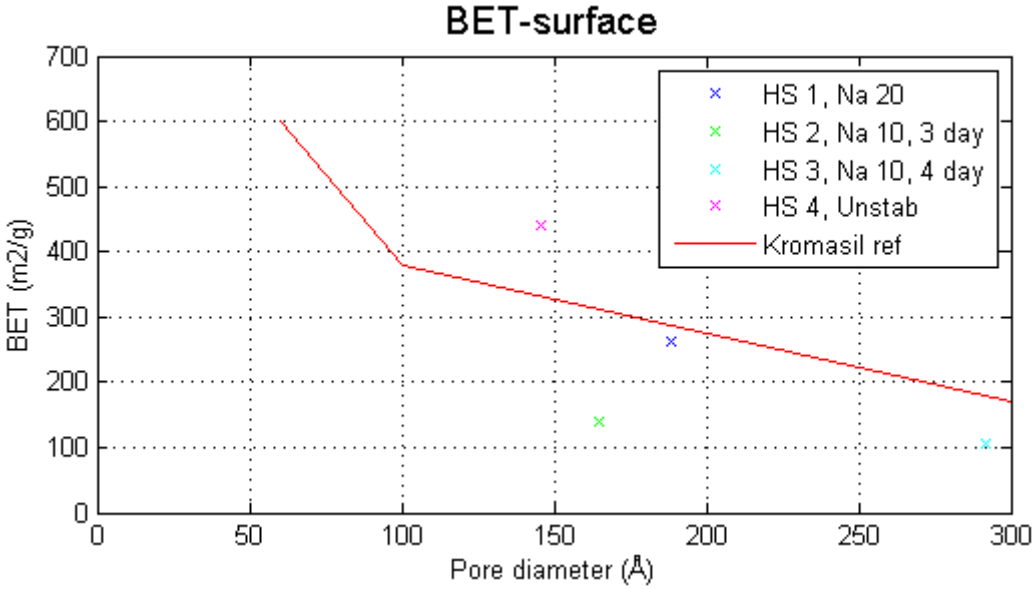

Figure 20: Specific surface area as a function of pore diameter.

In order to get small sol particles and still get a stable sol, a pH around 9 is desired. A study of possible bases for stabilising the sol was made to facilitate further work. Some suggestions are presented in table 7.

Table 7: Suggestions of possible bases that can be used to stabilise the silica sol.

Substance	pK_a	Amount (g/litre)	Solubility
4-(Methylamino)benzoic acid	5.04	13.8	Soluble
Pyridine	5.25	4.4	Miscible
2-Ethylpyridine	5.89	1.3	Soluble
2-Methylpyridine	5.97	1.0	Very soluble

6 Concluding remarks

The work in this project has shown that it is possible to use new emulsification methods to control the average particle diameter of porous silica gel particles. It is hence possible to produce gel materials with different average particle diameters compared with Kromasil products commercially available today.

The membrane emulsification method, as used in this project, needs to be more thoroughly evaluated and different types of membranes need to be tested. It should be considered to use a different set-up with a more controllable and even flow of the dispersed phase through the membrane.

Small average particle diameter can probably be achieved with the static mixer method. An almost linear relationship was found between the fluid velocity through the reducer in front of the mixing elements and the particle size. To be able to reach higher velocity and thus smaller particles, a set-up allowing higher pressures is necessary.

No real conclusions can be drawn from the results of the experiments aimed to produce particles with higher surface area. Too few experiments were made and the conditions, such as storage time and production method, were different for each experiment and are thus hard to compare.

7 Acknowledgement

I would like to thank the following people:

- My supervisor Anders Törncrona for giving me the opportunity to do my master thesis work at Eka Chemicals, Separation Products. Thank you for this interesting project with a lot of practical experiences.
- Professor Krister Holmberg for being my examiner.
- The production staff at Separation Products for all the nice coffee breaks and lunches and for helping me with the cleaning of the reactor. A special thanks to Carina Haarala, Sofia Friberg, Henric Fae and Lars-Åke Johansson for helping me perform the pilot scale experiments during two very long days.
- The staff working in the research lab for helping me out with my laboratory work, especially Peter Gidlund and Maria Forsberg.
- QC for running my analysis and helping me understand the analysis results.
- My team mates for Vårruset Lillemor, Barbro, Ulrika, Kristina and Maria. Thank you for the nice lunch walks with guidance trough Bohus and for the really nice evening with picnic in Slottsskogen.
- My three office mates, Emelie Öhgren, Albin Klint and Hafizur Rahman for nice chats and interesting discussions.
- Finally lots of thanks to my family and friends for all your support and encouragement.

8 References

[1] Berthod A. Silica: backbone material of liquid chromatographic column packings. Journal of Chromatography A. 1991;549:1–28.

[2] Unger KK. Porous silica. Journal of Chromatography Library. Amsterdam: Elsevier; 1979.

[3] Iler RK. The chemistry of silica. New York: Wiley; 1979.

[4] Brinker CJ, Scherer GW. Sol-gel science. Boston: Academic press, Inc; 1990.

[5] Peters DC. Dynamics of emulsification. In: Harnby N, Edwards MF, Nienow AW, editors. Mixing in the Process Industries. Oxford: Butterworth-Heinemann; 1997. p. 294–321.

[6] Groeneweg F, van Dieren F, Agterof WGM. Droplet break-up in a stirred water-in-oil emulsion in the presence of emulsifiers. Colloids and Surfaces A: Physicochemical and Engineering Aspects. 1994;91:207–214.

[7] Holmberg K, Jönsson B, Kronberg B, Lindman B. Surfactatnts and Polymers in Aqueous Solution. Chichester: Wiley & Sons, Ltd; 2002.

[8] Sinnott RK. Chemical Engineering Design. vol. 6 of Coulson & Richardson's Chemical Engineering. 4th ed. Butterworth-Heinemann; 2005.

[9] Tilton JN. Fluid and Particle Dynamics. In: Green DW, Perry RH, editors. Perry's Chemical Engineers' Handbook. 8th ed. New York: McGraw-Hill; 2008. .

[10] Edwards MF, Baker MR. A review of liquid mixing equipment. In: Harnby N, Edwards MF, Nienow AW, editors. Mixing in the Process Industries. Oxford: Butterworth-Heinemann; 1997. p. 118–136.

[11] Thakur RK, Vial C, Nigam KDP, Nauman EB, Djelveh G. Static Mixers in the Process Industries - A Review. Chemical Engineering Research and Design. 2003;81(7):787–826.

[12] Charcosset C, Limayem I, Fessi H. The membrane emulsification process - a review. Journal of Chemical Technology and Biotechnology. 2004;79(3):209–218.

[13] Joscelyne SM, Trägårdh G. Membrane emulsification - a literature review. Journal of Membrane Science. 2000;169(1):107–117.

[14] Kandori K, Kishi K, Ishikawa T. Formation mechanisms of monodispersed W/O emulsions by SPG filter emulsification method. Colloids and Surfaces. 1991;61:269–279.

[15] Nakashima T, Shimizu M, Kukizaki M. Particle control of emulsion by membrane emulsification and its applications. Advanced Drug Delivery Reviews. 2000;45(1):47–56.

[16] Xu Y. Particle size analyses of porous silica and hybrid silica chromatographic support particles: Comparison of flow/hyperlayer field-flow fractionation with scanning electron microscopy, electrical sensing zone, and static light scattering. Journal of Chromatography A. 2008;1191(1-2):40–56.

[17] Sing KSW. Reporting physisorption data for gas/solid systems with special reference to the determination of surface area and porosity. Pure and Applied Chemistry. 1982;54(11):2201–2218.

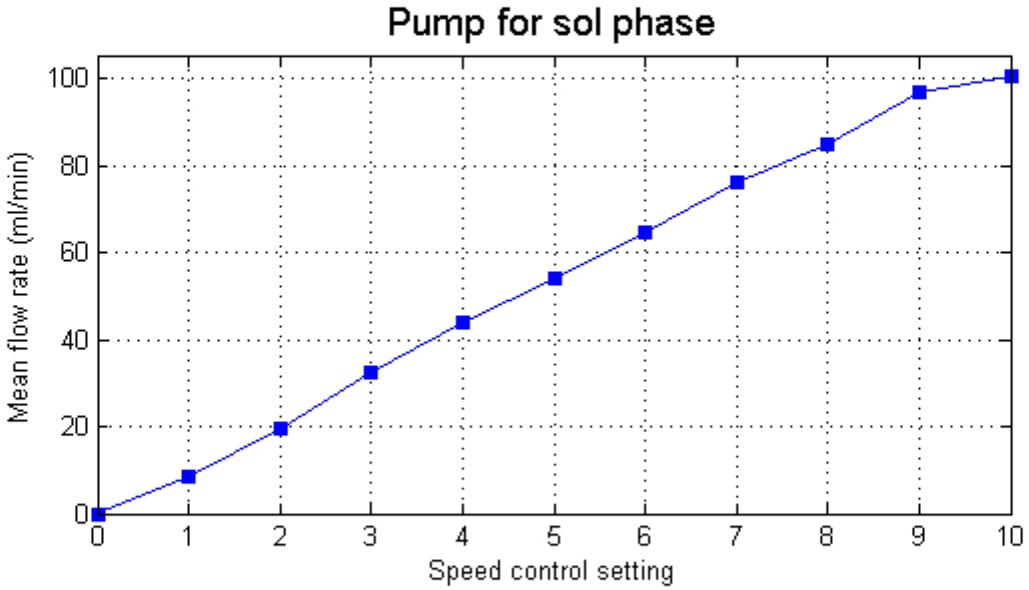
Pump for sol phase
Mean flow rate (ml/min)
Speed control setting
0
20
40
60
80
100
0
1
2
3
4
5
6
7
8
9
10

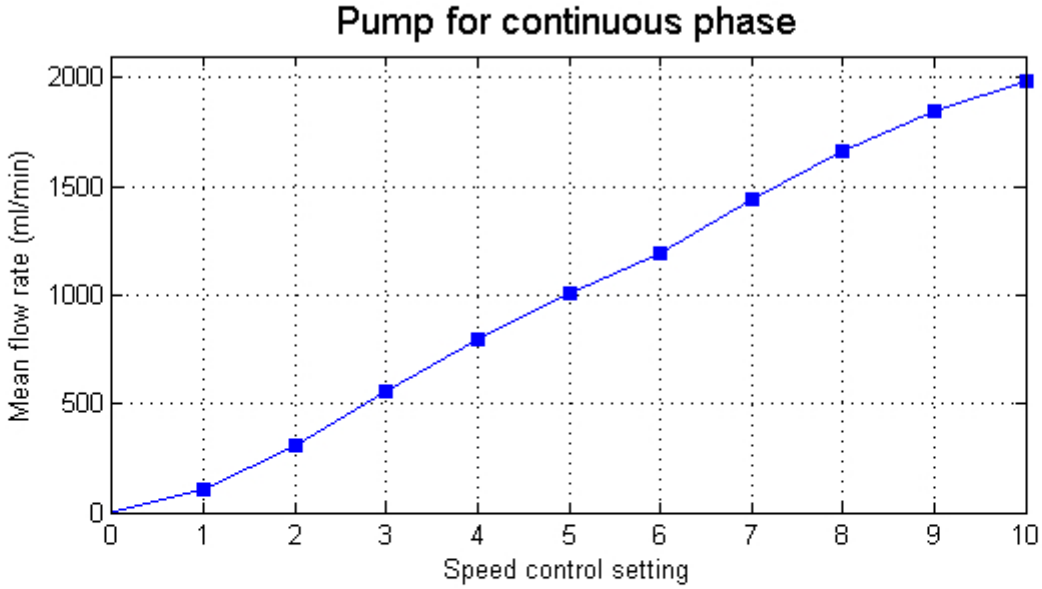
Pump for continuous phase
Mean flow rate (ml/min)
Speed control setting
0
500
1000
1500
2000
0
1
2
3
4
5
6
7
8
9
10

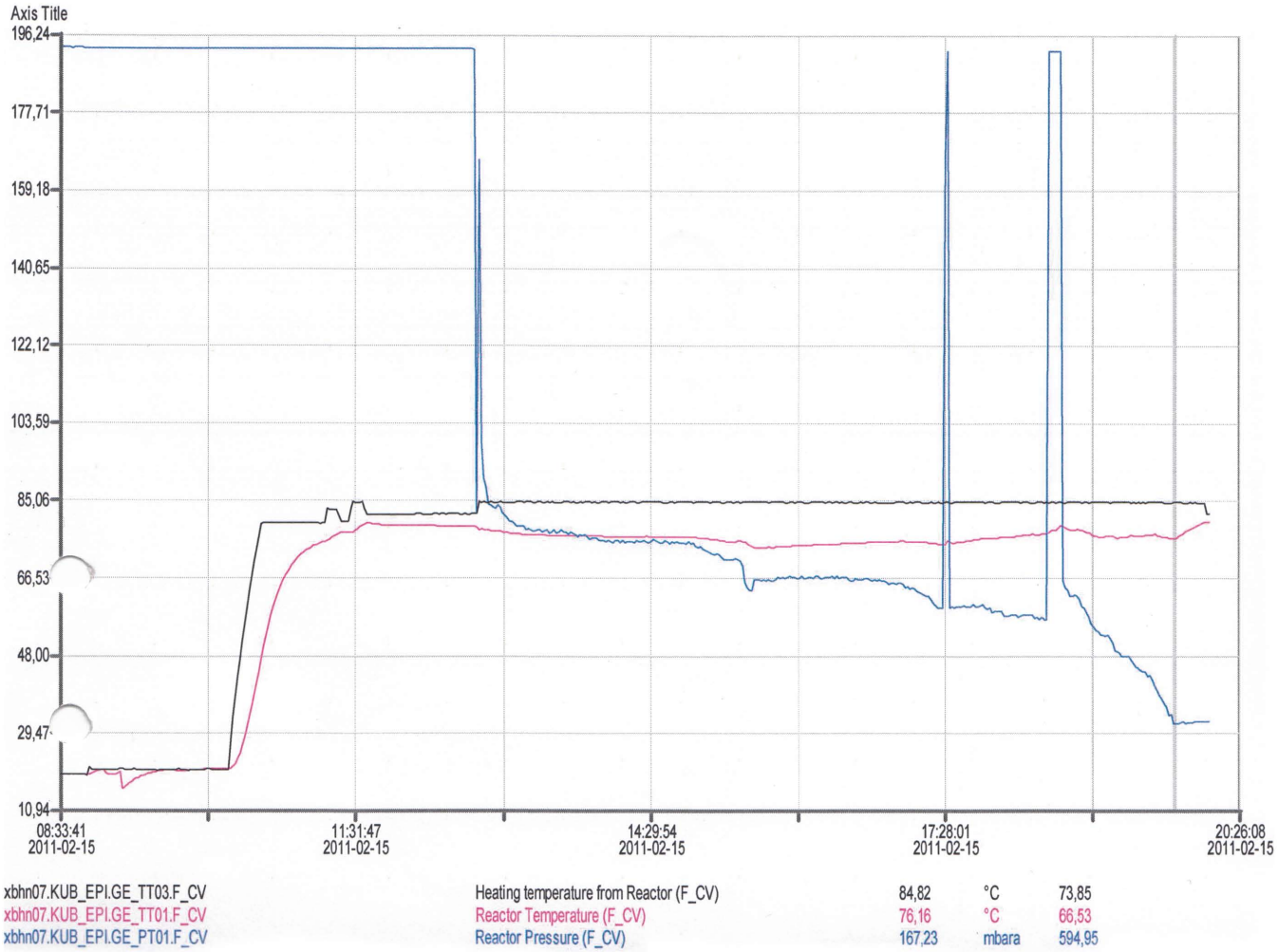
Axis Title
196,24
177,71
159,18
140,65
122,12
103,59
85,06
66,53
48,00
29,47
10,94
08:33:41
2011-02-15
11:31:47
2011-02-15
14:29:54
2011-02-15
17:28:01
2011-02-15
20:26:08
2011-02-15
xbhn07.KUB_EPI.GE_TT03.F_CV
Heating temperature from Reactor (F_CV)
84,82
°C
73,85
xbhn07.KUB_EPI.GE_TT01.F_CV
Reactor Temperature (F_CV)
76,16
°C
66,53
xbhn07.KUB_EPI.GE_PT01.F_CV
Reactor Pressure (F_CV)
167,23
mbara
594,95

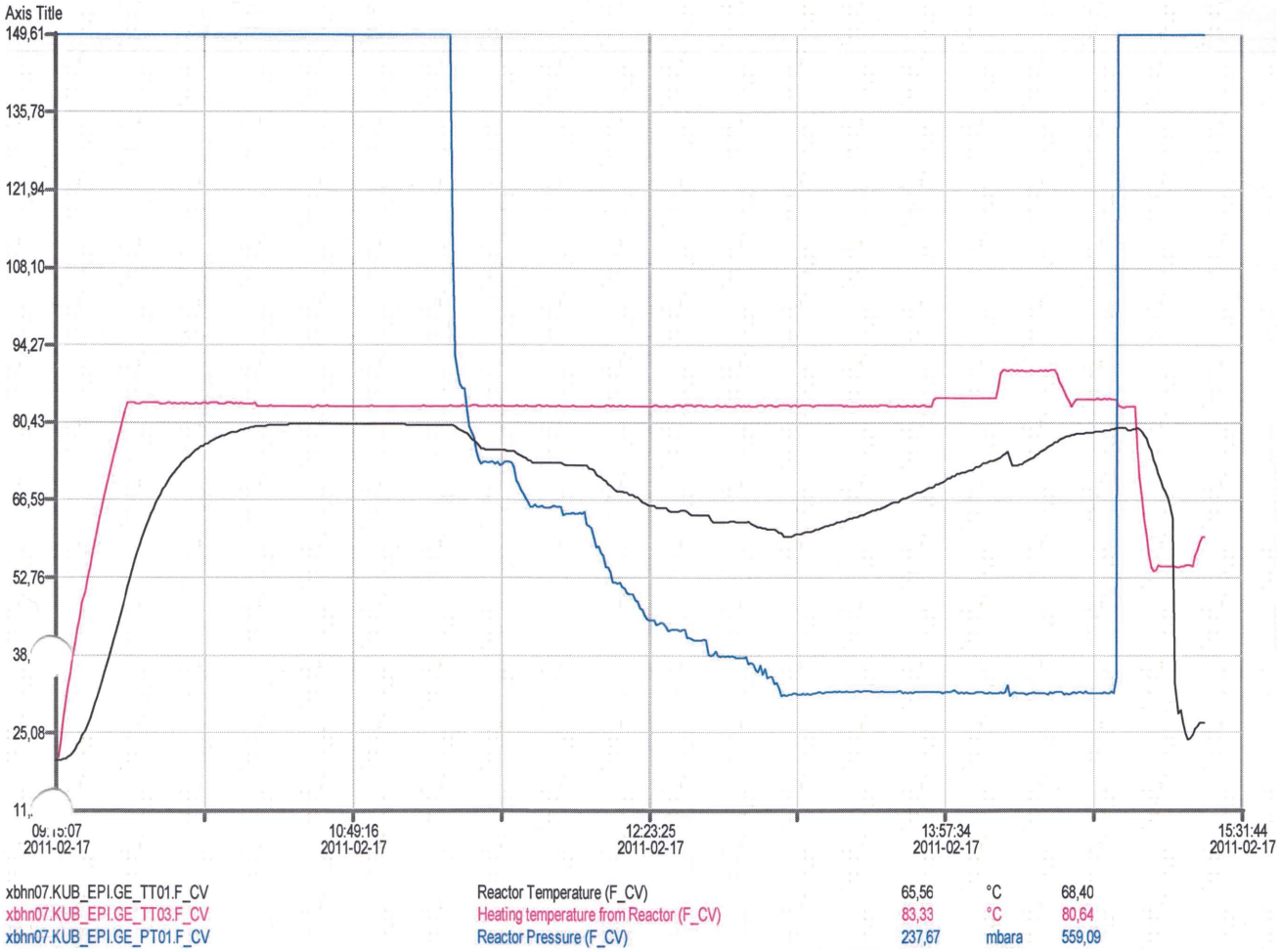
Axis Title
149,61
135,78
121,94
108,10
94,27
80,43
66,59
52,76
38,
25,08
11,
10:49:16
2011-02-17
12:23:25
2011-02-17
13:57:34
2011-02-17
15:31:44
2011-02-17
xbhn07.KUB_EPI.GE_TT01.F_CV
Reactor Temperature (F_CV)
65,56
°C
68,40
xbhn07.KUB_EPI.GE_TT03.F_CV
Heating temperature from Reactor (F_CV)
83,33
°C
80,64
xbhn07.KUB_EPI.GE_PT01.F_CV
Reactor Pressure (F_CV)
237,67
mbara
559,09

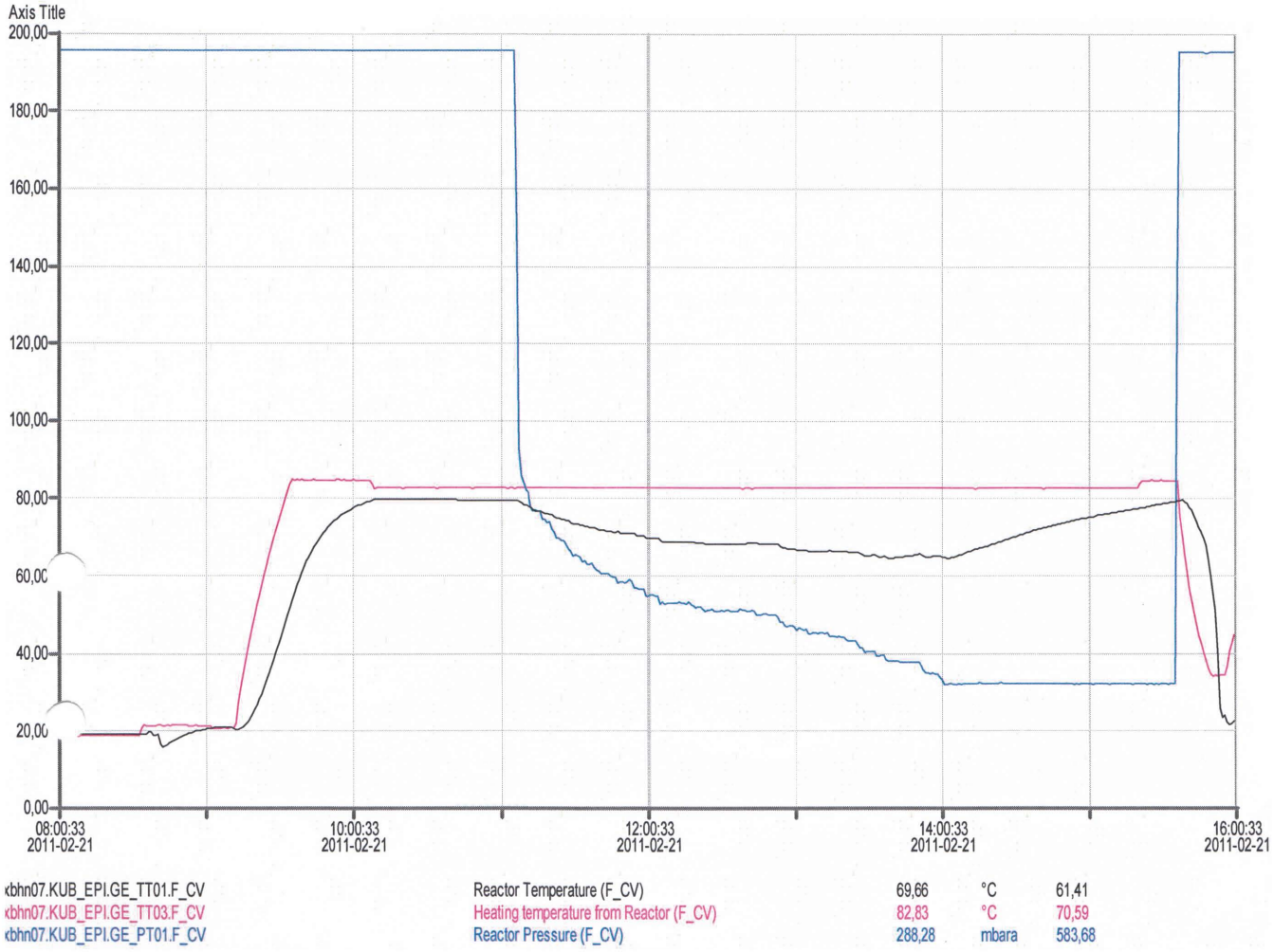
Axis Title
200,00
180,00
160,00
140,00
120,00
100,00
80,00
60,00
40,00
20,00
0,00
08:00:33
2011-02-21
10:00:33
2011-02-21
12:00:33
2011-02-21
14:00:33
2011-02-21
16:00:33
2011-02-21
‹bhn07.KUB_EPI.GE_TT01.F_CV
‹bhn07.KUB_EPI.GE_TT03.F_CV
‹bhn07.KUB_EPI.GE_PT01.F_CV
Reactor Temperature (F_CV) 69,66 °C 61,41
Heating temperature from Reactor (F_CV) 82,83 °C 70,59
Reactor Pressure (F_CV) 288,28 mbara 583,68


xis Title
97,27
79,14
61,01
42,88
24,76
06,63
88,50
70,37
52,24
34,11
15,98
04:44:04
2011-02-24
07:44:28
2011-02-24
10:44:52
2011-02-24
13:45:16
2011-02-24
16:45:41
2011-02-24
nn07.KUB_EPI.GE_TT01.F_CV
Reactor Temperature (F_CV)
77,07
°C
53,43
nn07.KUB_EPI.GE_TT03.F_CV
Heating temperature from Reactor (F_CV)
84,79
°C
61,52
nn07.KUB_EPI.GE_PT01.F_CV
Reactor Pressure (F_CV)
394,64
mbara
734,92

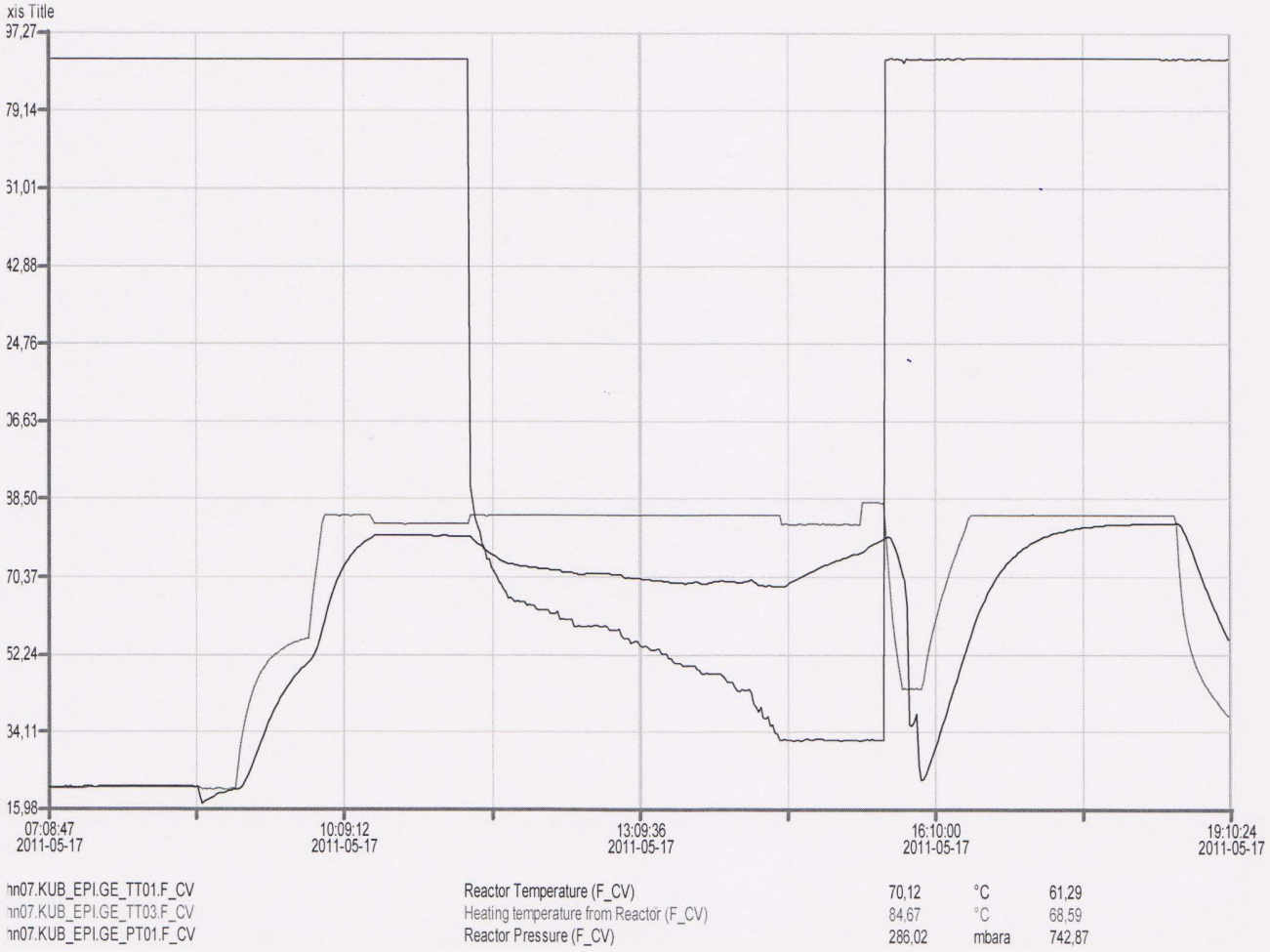
xis Title
97,27
79,14
31,01
42,88
24,76
06,63
88,50
70,37
52,24
34,11
15,98
07:08:47
2011-05-17
10:09:12
2011-05-17
13:09:36
2011-05-17
16:10:00
2011-05-17
19:10:24
2011-05-17
hn07.KUB_EPI.GE_TT01.F_CV
hn07.KUB_EPI.GE_TT03.F_CV
hn07.KUB_EPI.GE_PT01.F_CV
Reactor Temperature (F_CV)
Heating temperature from Reactor (F_CV)
Reactor Pressure (F_CV)
70,12 °C 61,29
84,67 °C 68,59
286,02 mbara 742,87

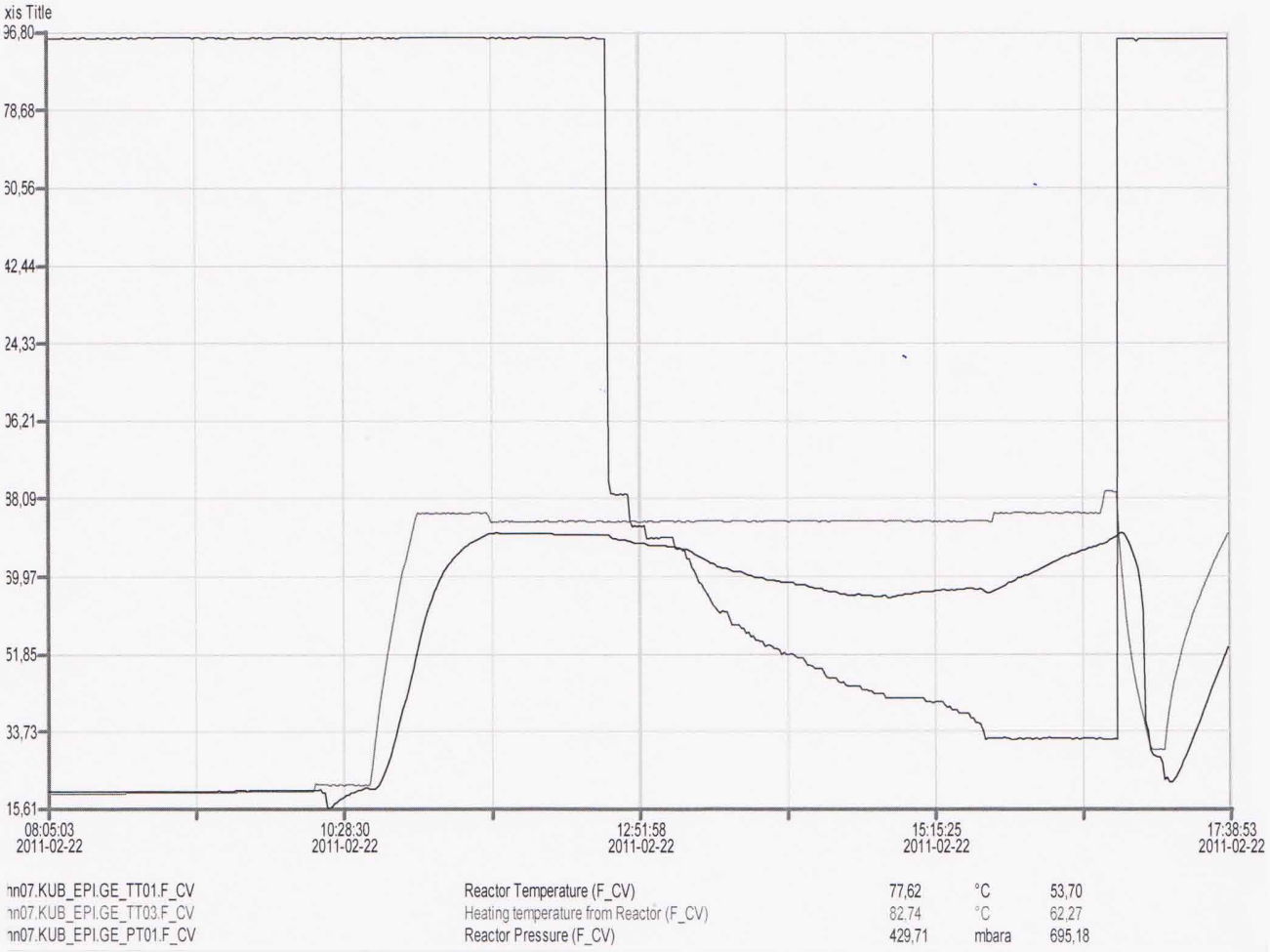
xis Title
96,80
78,68
30,56
42,44
24,33
36,21
38,09
39,97
51,85
33,73
15,61
08:05:03
2011-02-22
10:28:30
2011-02-22
12:51:58
2011-02-22
15:15:25
2011-02-22
17:38:53
2011-02-22
nn07.KUB_EPI.GE_TT01.F_CV
Reactor Temperature (F_CV)
77,62
°C
53,70
nn07.KUB_EPI.GE_TT03.F_CV
Heating temperature from Reactor (F_CV)
82,74
°C
62,27
nn07.KUB_EPI.GE_PT01.F_CV
Reactor Pressure (F_CV)
429,71
mbara
695,18


xis Title
97,27
79,14
31,01
42,88
24,76
06,63
88,50
70,37
52,24
34,11
15,98
07:05:33
2011-05-16
10:05:58
2011-05-16
13:06:22
2011-05-16
16:06:46
2011-05-16
19:07:10
2011-05-16
nn07.KUB_EPI.GE_TT01.F_CV
Reactor Temperature (F_CV)
70,13
°C
57,12
nn07.KUB_EPI.GE_TT03.F_CV
Heating temperature from Reactor (F_CV)
84,67
°C
65,97
nn07.KUB_EPI.GE_PT01.F_CV
Reactor Pressure (F_CV)
293,53
mbara
734,89


is Title
,54
,50
,46
,43
,39
,35
,31
,27
,23
,80
,84
04:21:27
2011-04-27
08:59:47
2011-04-27
13:38:08
2011-04-27
18:16:29
2011-04-27
22:54:50
2011-04-27
nn07.KUB_EPI.TI-020.F_CV
nn07.KUB_EPI.PI-053.F_CV
Temp reaktor 5301 (F_CV)
Tryck i reaktor 5301 (F_CV)
74,04
-0,64
°C
BAR
44,95
-0,21

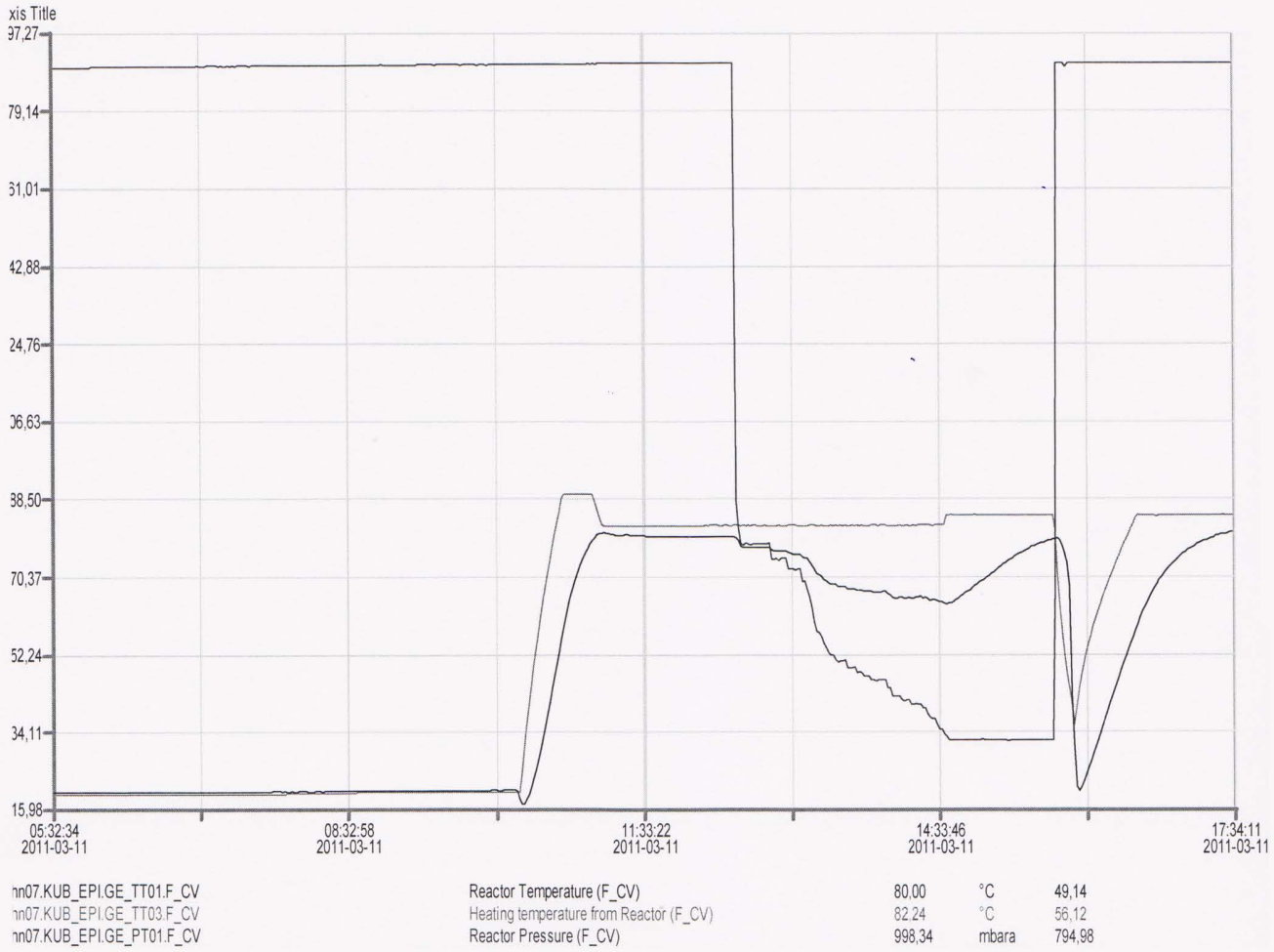
xis Title
97,27
79,14
61,01
42,88
24,76
06,63
88,50
70,37
52,24
34,11
15,98
05:32:34
2011-03-11
08:32:58
2011-03-11
11:33:22
2011-03-11
14:33:46
2011-03-11
17:34:11
2011-03-11
nn07.KUB_EPI.GE_TT01.F_CV
Reactor Temperature (F_CV)
80,00
°C
49,14
nn07.KUB_EPI.GE_TT03.F_CV
Heating temperature from Reactor (F_CV)
82,24
°C
56,12
nn07.KUB_EPI.GE_PT01.F_CV
Reactor Pressure (F_CV)
998,34
mbara
794,98

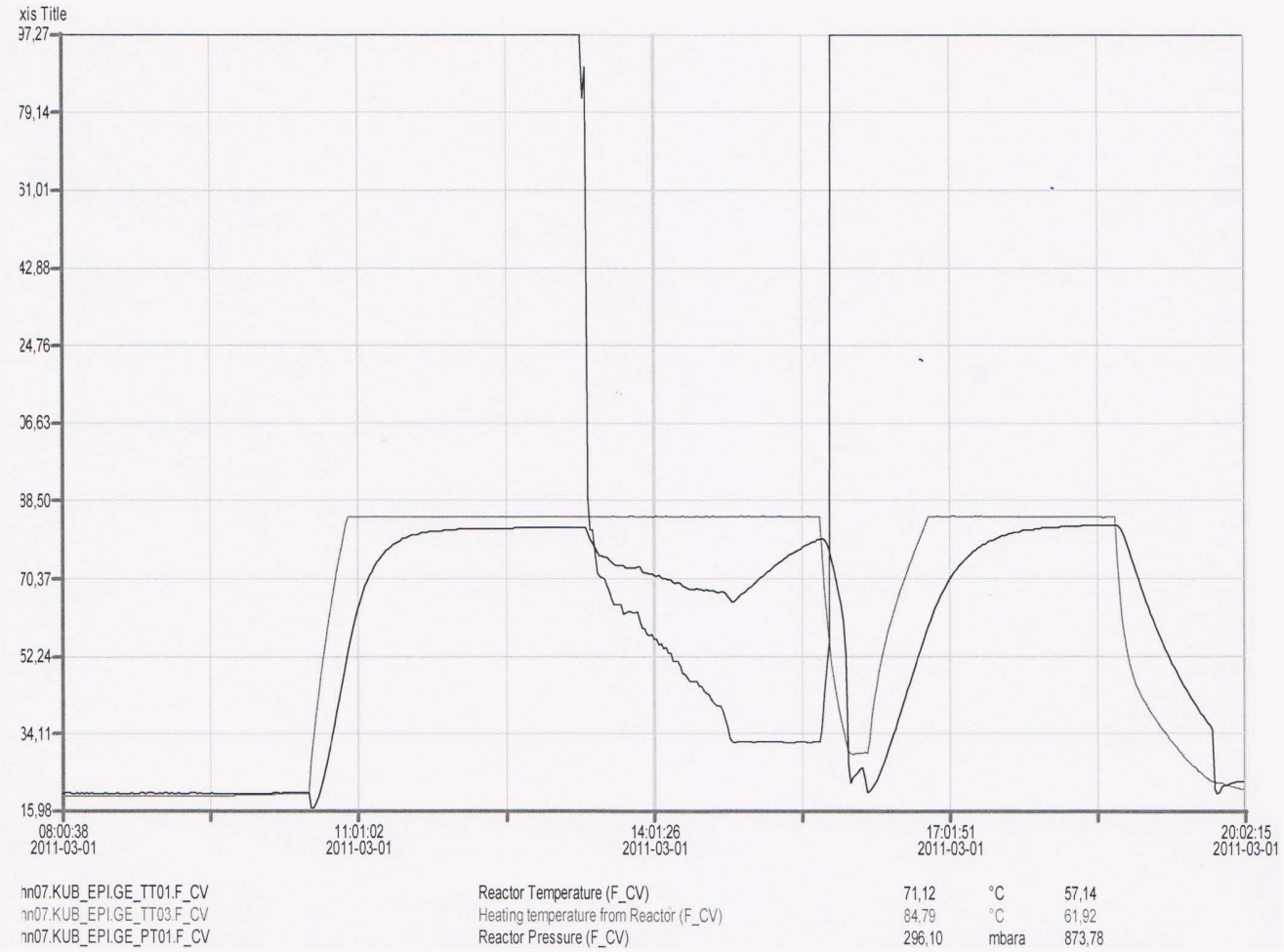
xis Title
97,27
79,14
31,01
42,88
24,76
06,63
88,50
70,37
52,24
34,11
15,98
08:00:38
2011-03-01
11:01:02
2011-03-01
14:01:26
2011-03-01
17:01:51
2011-03-01
20:02:15
2011-03-01
nn07.KUB_EPI.GE_TT01.F_CV
nn07.KUB_EPI.GE_TT03.F_CV
nn07.KUB_EPI.GE_PT01.F_CV
Reactor Temperature (F_CV)
Heating temperature from Reactor (F_CV)
Reactor Pressure (F_CV)
71,12 °C 57,14
84,79 °C 61,92
296,10 mbara 873,78

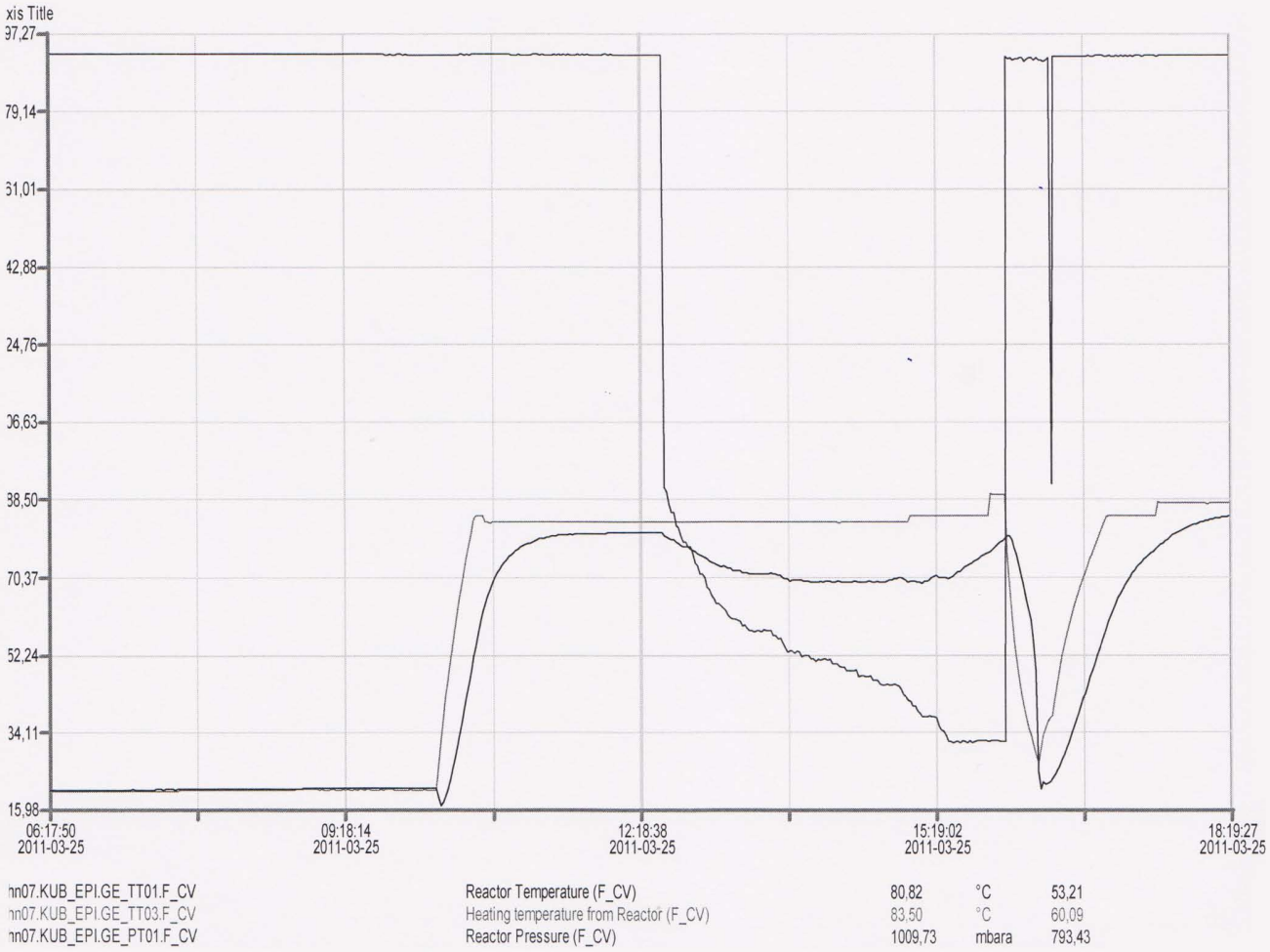
xis Title
97,27
79,14
31,01
42,88
24,76
06,63
88,50
70,37
52,24
34,11
15,98
06:17:50
2011-03-25
09:18:14
2011-03-25
12:18:38
2011-03-25
15:19:02
2011-03-25
18:19:27
2011-03-25
nn07.KUB_EPI.GE_TT01.F_CV
Reactor Temperature (F_CV)
80,82
°C
53,21
nn07.KUB_EPI.GE_TT03.F_CV
Heating temperature from Reactor (F_CV)
83,50
°C
60,09
nn07.KUB_EPI.GE_PT01.F_CV
Reactor Pressure (F_CV)
1009,73
mbara
793,43

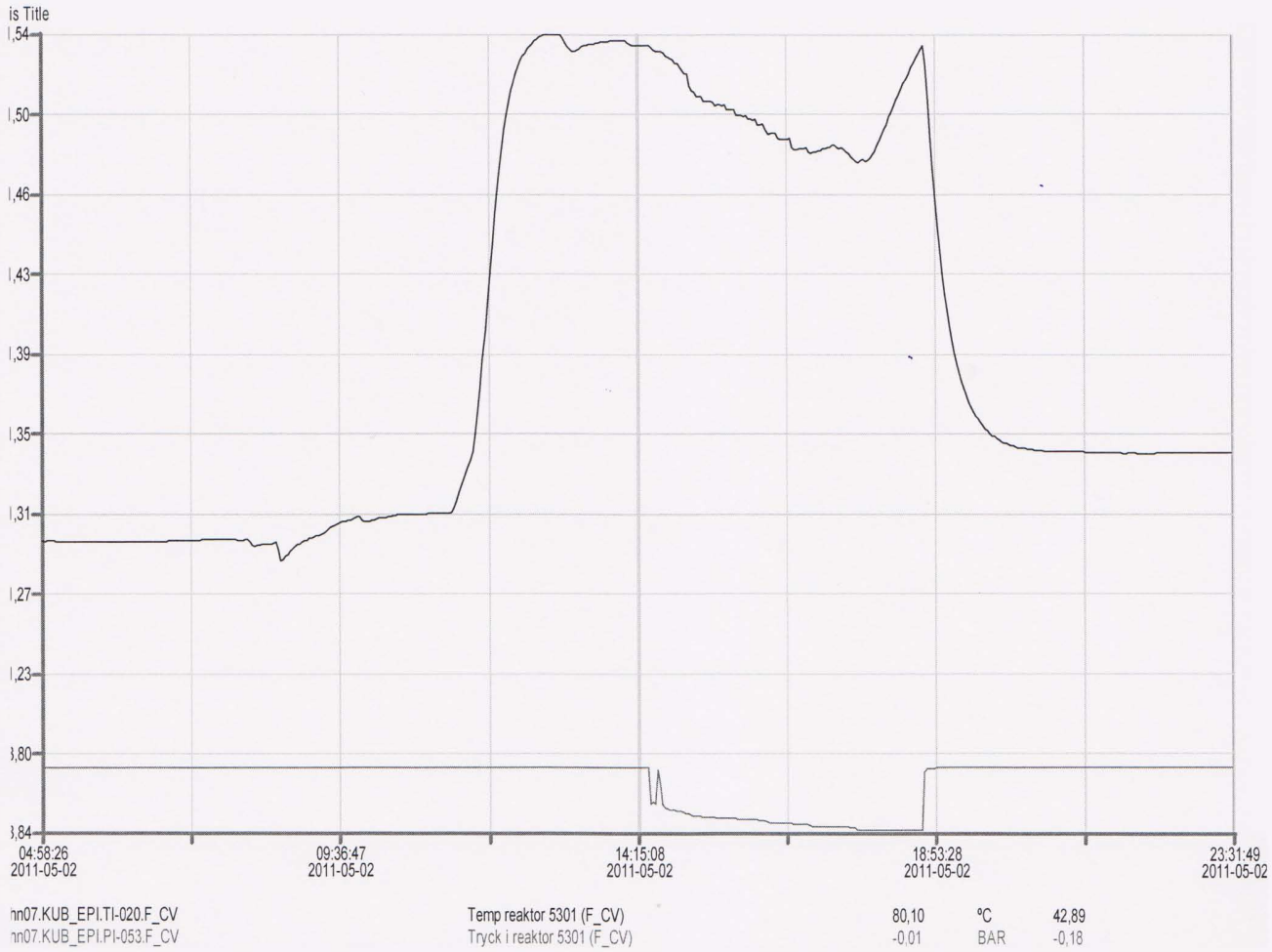
is Title
,54
,50
,46
,43
,39
,35
,31
,27
,23
,80
,84
04:58:26
2011-05-02
09:36:47
2011-05-02
14:15:08
2011-05-02
18:53:28
2011-05-02
23:31:49
2011-05-02
nn07.KUB_EPI.TI-020.F_CV
Temp reaktor 5301 (F_CV)
80,10
°C
42,89
nn07.KUB_EPI.PI-053.F_CV
Tryck i reaktor 5301 (F_CV)
-0,01
BAR
-0,18

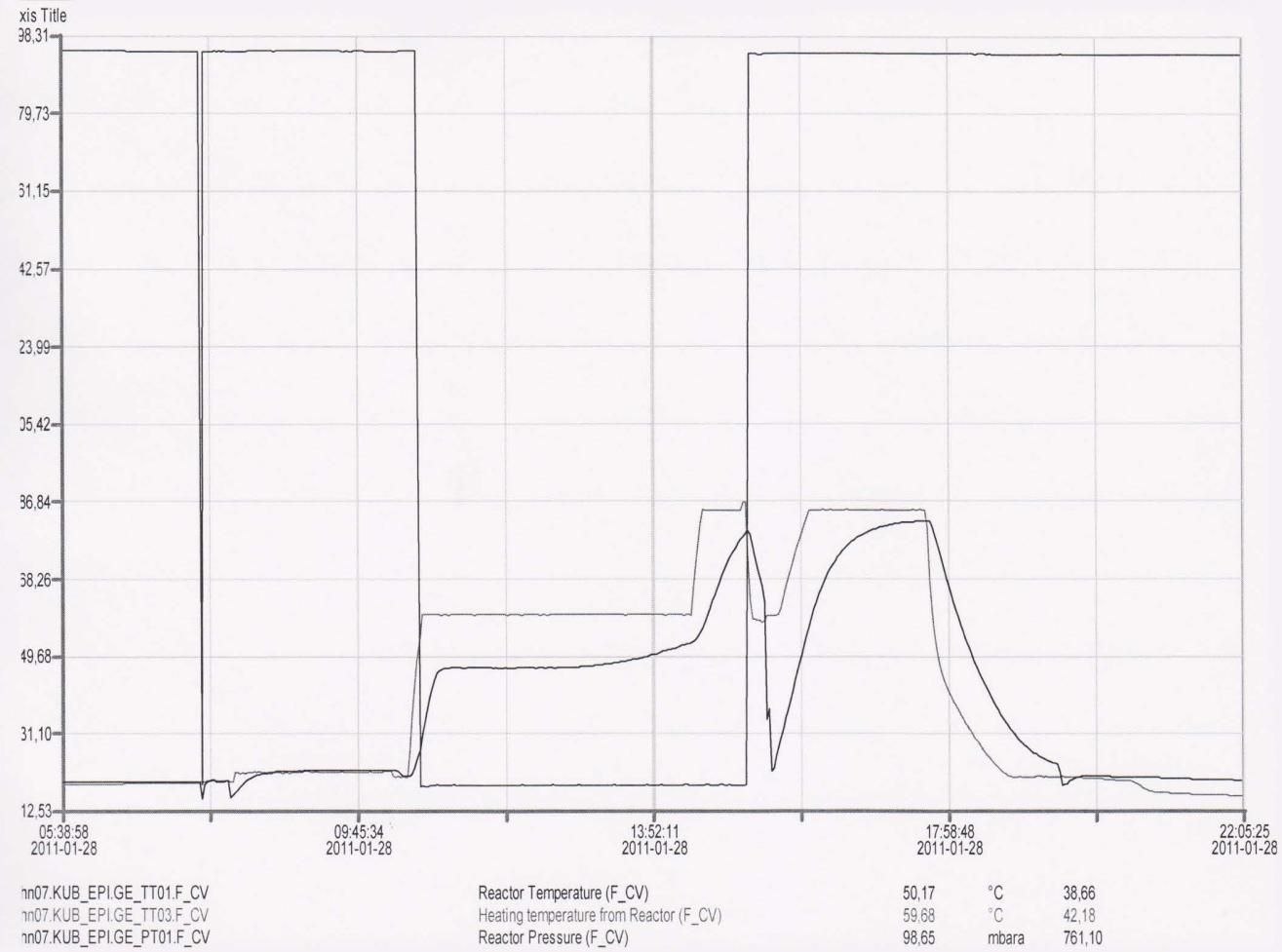
xis Title
98,31
79,73
31,15
42,57
23,99
05,42
86,84
68,26
49,68
31,10
12,53
05:38:58
2011-01-28
09:45:34
2011-01-28
13:52:11
2011-01-28
17:58:48
2011-01-28
22:05:25
2011-01-28
nn07.KUB_EPI.GE_TT01.F_CV
nn07.KUB_EPI.GE_TT03.F_CV
nn07.KUB_EPI.GE_PT01.F_CV
Reactor Temperature (F_CV)
Heating temperature from Reactor (F_CV)
Reactor Pressure (F_CV)
50,17 °C 38,66
59,68 °C 42,18
98,65 mbara 761,10

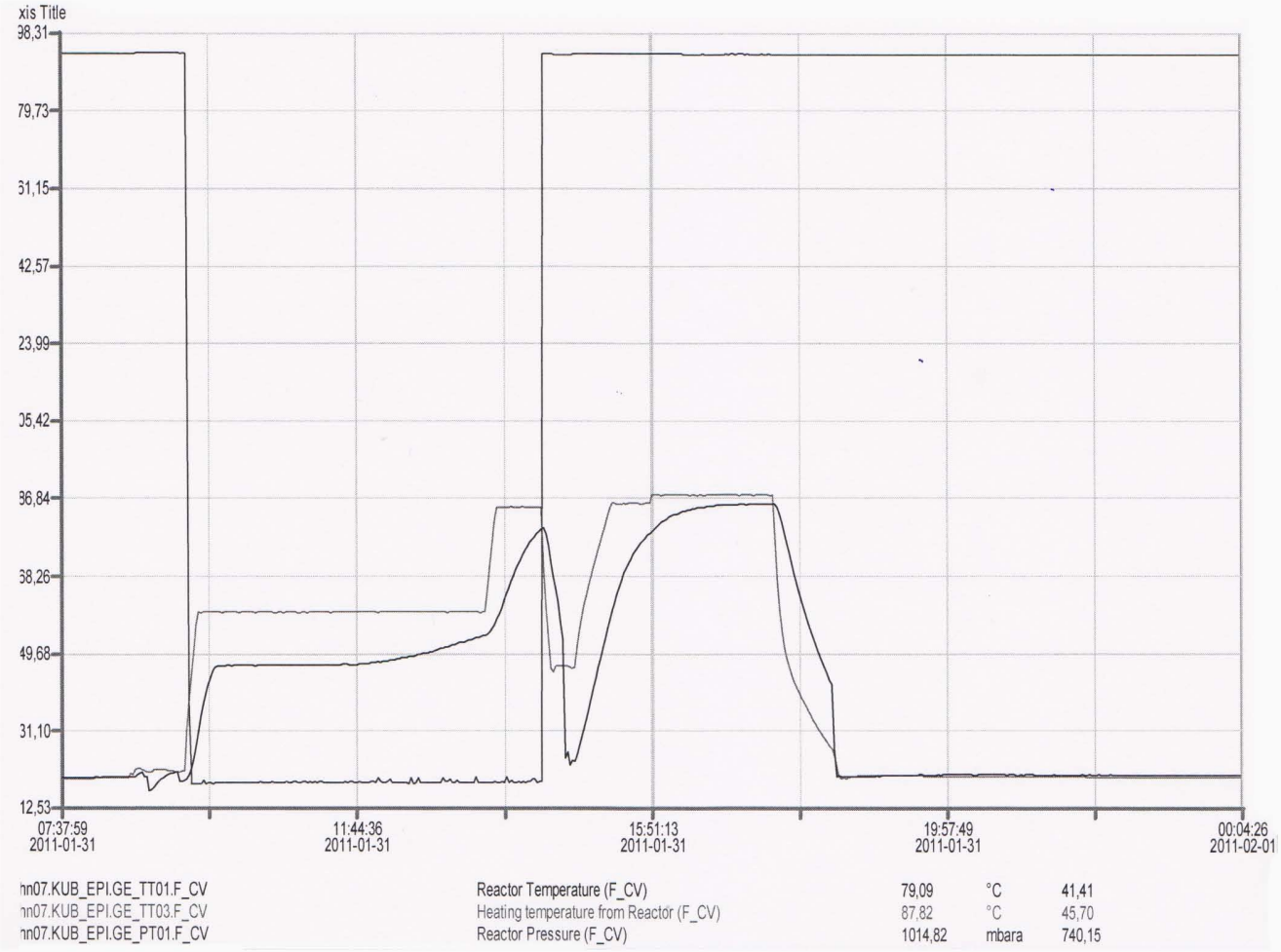
xis Title
98,31
79,73
31,15
42,57
23,99
05,42
86,84
68,26
49,68
31,10
12,53
07:37:59
2011-01-31
11:44:36
2011-01-31
15:51:13
2011-01-31
19:57:49
2011-01-31
00:04:26
2011-02-01
hn07.KUB_EPI.GE_TT01.F_CV
Reactor Temperature (F_CV)
79,09
°C
41,41
hn07.KUB_EPI.GE_TT03.F_CV
Heating temperature from Reactor (F_CV)
87,82
°C
45,70
hn07.KUB_EPI.GE_PT01.F_CV
Reactor Pressure (F_CV)
1014,82
mbara
740,15

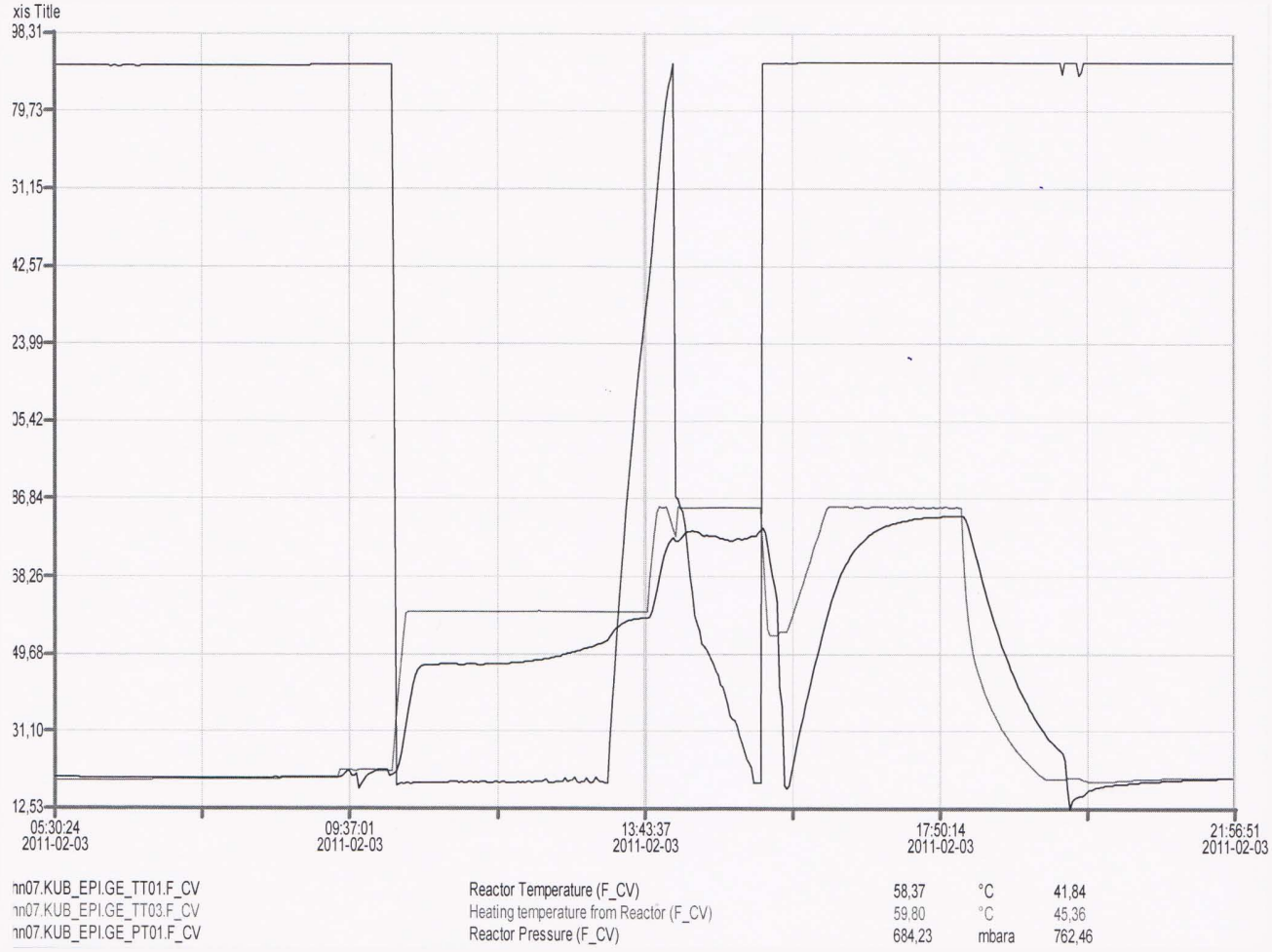
xis Title
98,31
79,73
61,15
42,57
23,99
05,42
86,84
68,26
49,68
31,10
12,53
05:30:24
2011-02-03
09:37:01
2011-02-03
13:43:37
2011-02-03
17:50:14
2011-02-03
21:56:51
2011-02-03
nn07.KUB_EPI.GE_TT01.F_CV
Reactor Temperature (F_CV)
58,37
°C
41,84
nn07.KUB_EPI.GE_TT03.F_CV
Heating temperature from Reactor (F_CV)
59,80
°C
45,36
nn07.KUB_EPI.GE_PT01.F_CV
Reactor Pressure (F_CV)
684,23
mbara
762,46

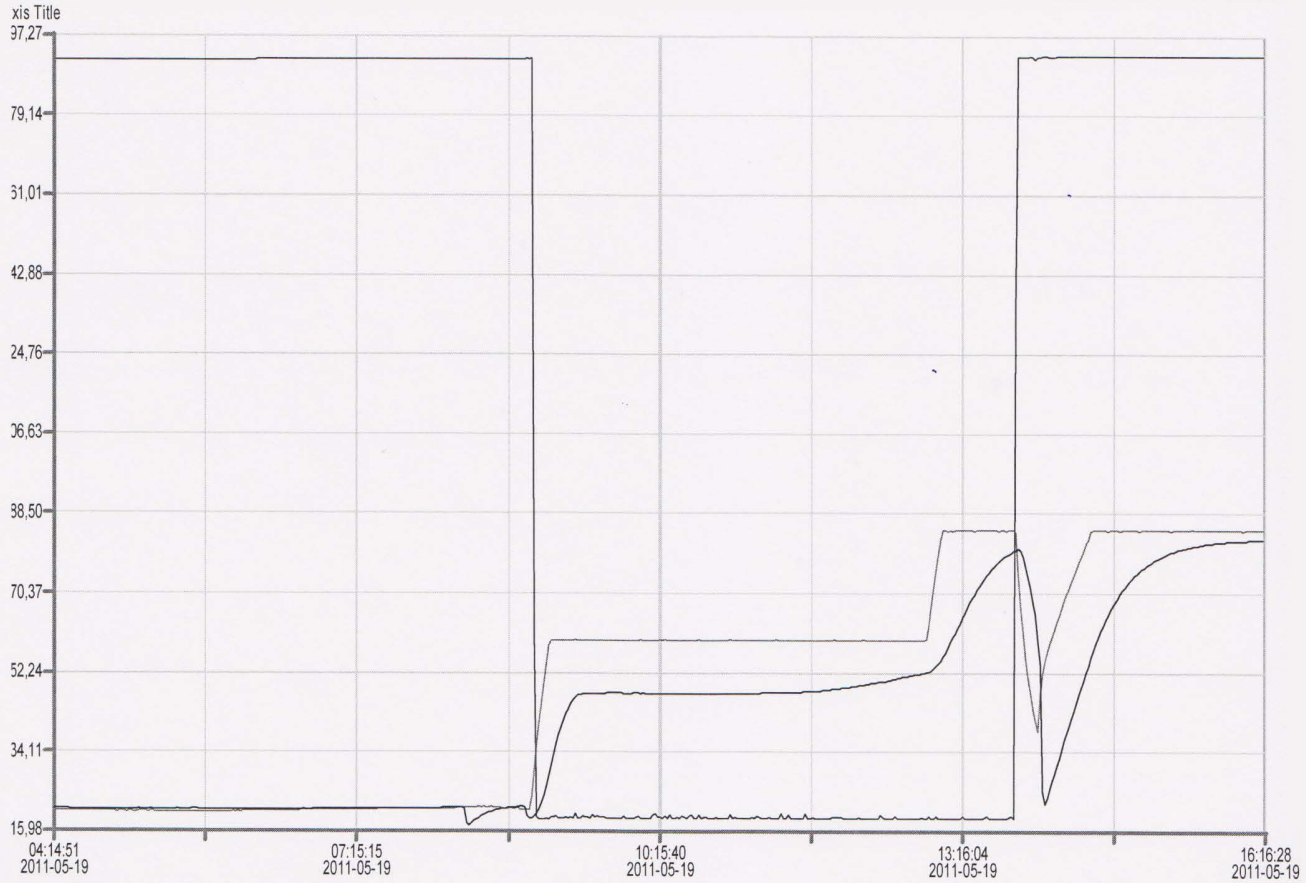
xis Title
97,27
79,14
31,01
42,88
24,76
06,63
88,50
70,37
52,24
34,11
15,98
04:14:51
2011-05-19
07:15:15
2011-05-19
10:15:40
2011-05-19
13:16:04
2011-05-19
16:16:28
2011-05-19
nn07.KUB_EPI.GE_TT01.F_CV
nn07.KUB_EPI.GE_TT03.F_CV
nn07.KUB_EPI.GE_PT01.F_CV
Reactor Temperature (F_CV)
Heating temperature from Reactor (F_CV)
Reactor Pressure (F_CV)
47,47 °C 42,54
59,76 °C 49,64
101,22 mbara 647,14

Extend5

FPIA-3000

14/03/2011

sysmex

Tested	
ReAnalyzed	14/03/2011 12:48:27
Measurer name	
ReAnalyzed By	Manager
SOP	
Sample name	XKR007_Merge
Sample number	1
Sample type	10 - 30 µm
Comment	5,2mg / 20ml
Power Field	HPF
Count method	Stop By Counts
Sheath Liquid	Particle Sheath

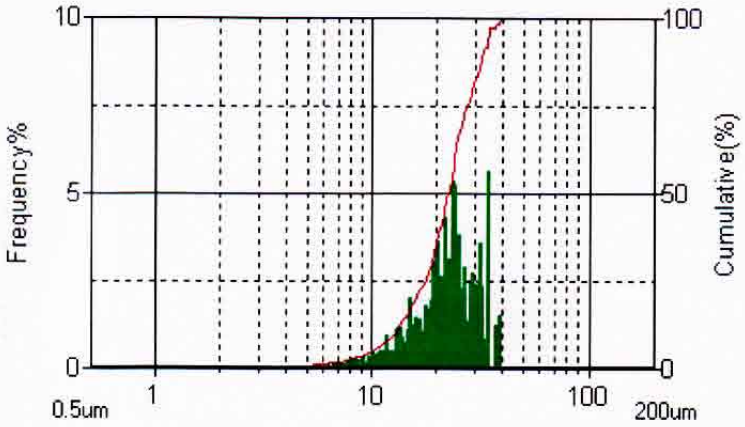

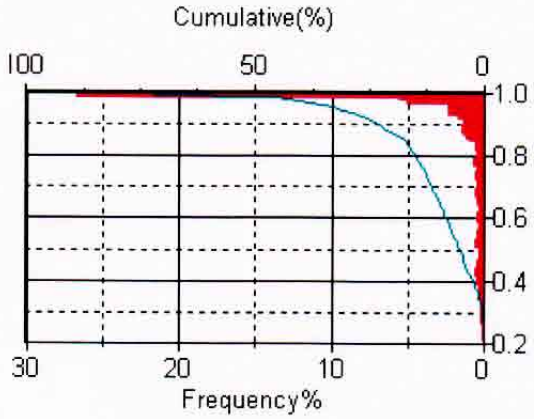

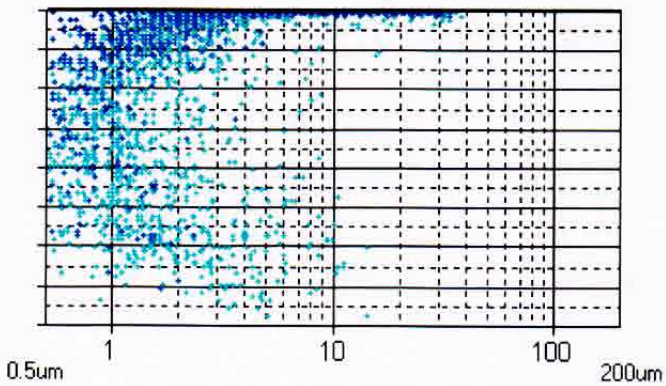

Particle dia

--- <= CE Diameter(V) < 200.0

Particle shap

--- <= Circularity <= ---

	CE Diameter(V)	Circularity			
Mean :	22.535	Mean :	0.914	Density :	782
SD :	7.381	SD :	0.160	Large(%) :	******
CV :	32.75	CV :	17.50	Middle(%) :	******
Mode :	34.307	Mode :	1.000	Small(%) :	******
Lower% :	12.811	Lower% :	0.667	Selected(%) :	100.00
50% :	22.507	50% :	0.992	Analyzed(#) :	6000
Upper% :	32.717	Upper% :	1.000	Selected(#) :	5406

div 90/10 = 2,55

20um

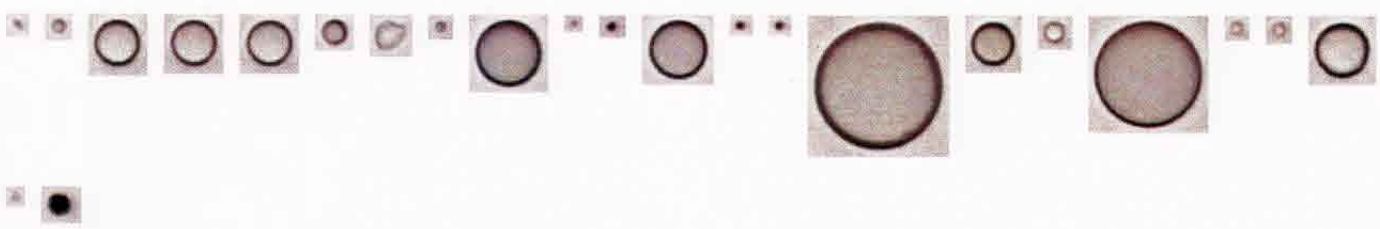

110314/ULA

FPIA-3000

Standard

14/03/2011

sysmex

Tested	
ReAnalyzed	14/03/2011 10:08:15
Measurer name	
ReAnalyzed By	Manager
SOP	
Sample name	XKR008_Merge
Sample number	1
Sample type	10 - 60 µm
Comment	5,2mg / 20ml
Power Field	LPF
Count method	Stop By Counts
Sheath Liquid	Particle Sheath

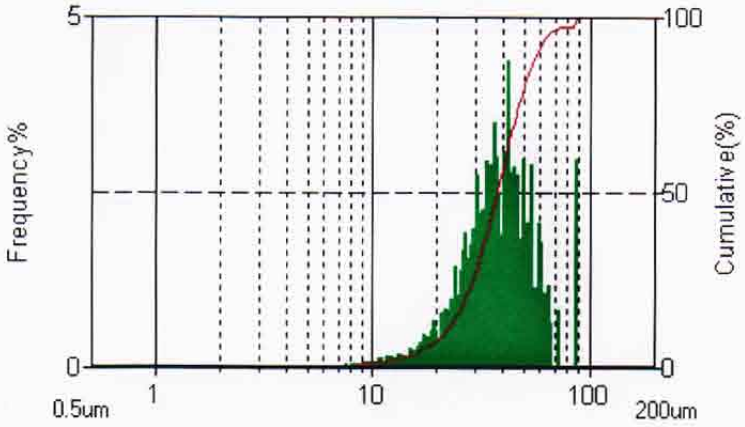

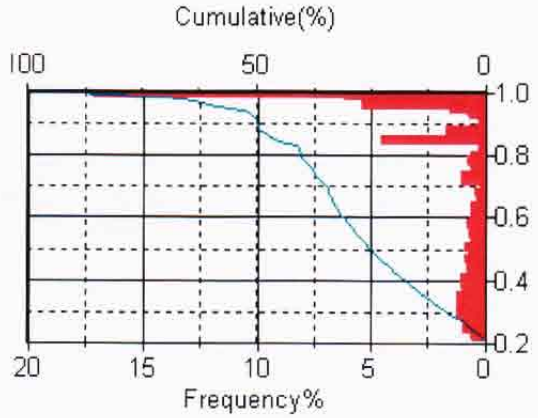

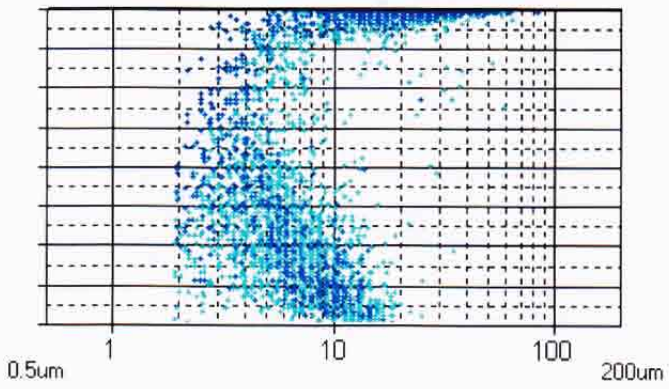

Particle dia

0.500 <= CE Diameter(V) < 200.0

Particle shap

0.200 <= Circularity <= 1.000

	CE Diameter(V)	Circularity			
Mean :	39.329	Mean :	0.763	Density :	106
SD :	15.117	SD :	0.270	Large(%) :	0.00
CV :	38.44	CV :	35.45	Middle(%) :	100.00
Mode :	42.412	Mode :	0.995	Small(%) :	0.00
Lower% :	21.868	Lower% :	0.318	Selected(%) :	100.00
50% :	37.629	50% :	0.914	Analyzed(#) :	6000
Upper% :	58.267	Upper% :	1.000	Selected(#) :	6000

dv90/10 = 2,66

100um

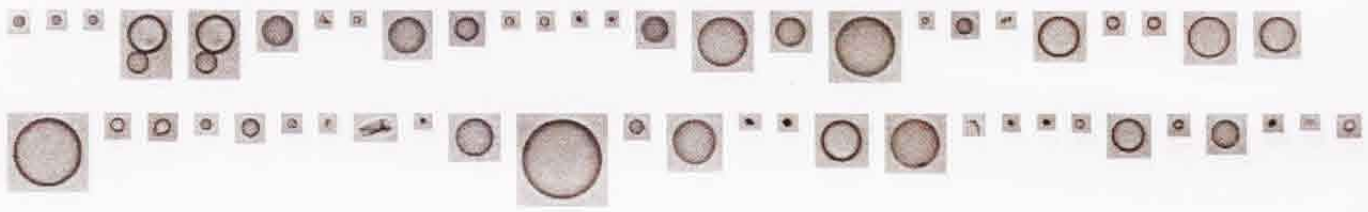

110314 /ULA

FPIA-3000

sysmex

Extend5

14/03/2011

Tested	
ReAnalyzed	14/03/2011 14:34:36
Measurer name	
ReAnalyzed By	Manager
SOP	
Sample name	XKR009_Merge
Sample number	1
Sample type	10 - 30 µm
Comment	5,2mg / 20ml
Power Field	HPF
Count method	Stop By Counts
Sheath Liquid	Particle Sheath

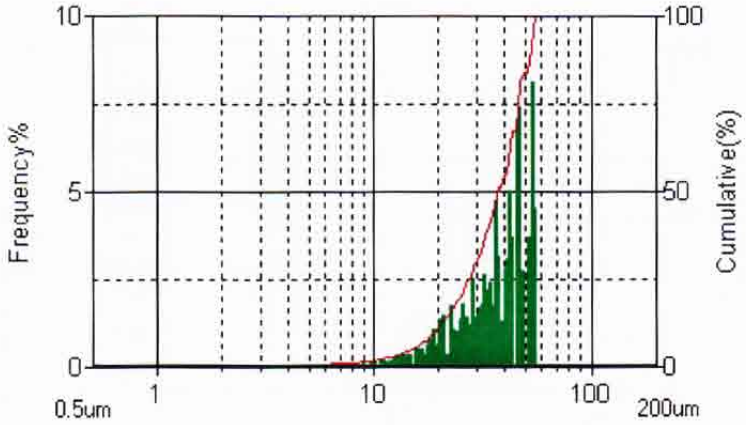

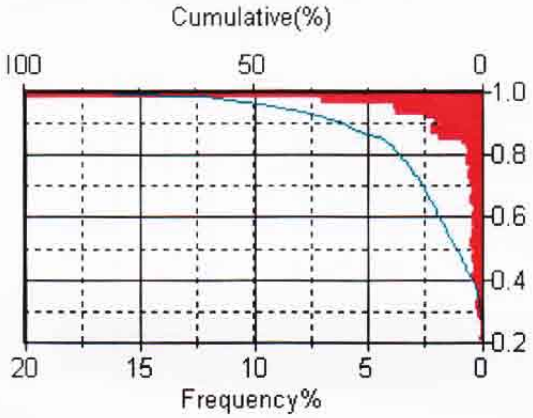

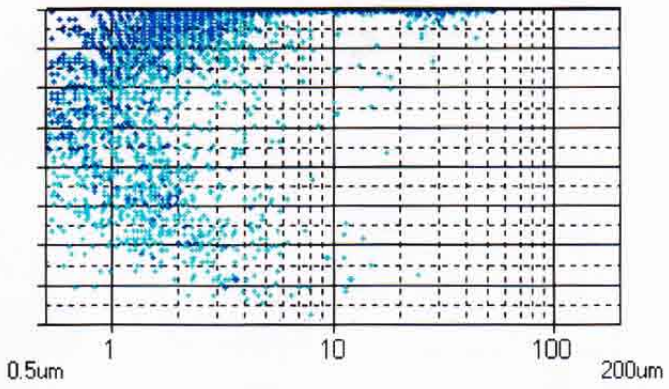

Particle dia

--- <= CE Diameter(V) < 200.0

Particle shap

--- <= Circularity <= ---

	CE Diameter(V)	Circularity			
Mean :	36.690	Mean :	0.894	Density :	399
SD :	12.386	SD :	0.164	Large(%) :	******
CV :	33.76	CV :	18.33	Middle(%) :	******
Mode :	53.841	Mode :	0.995	Small(%) :	******
Lower% :	19.055	Lower% :	0.622	Selected(%) :	100.00
50% :	37.573	50% :	0.971	Analyzed(#) :	6000
Upper% :	53.172	Upper% :	1.000	Selected(#) :	5200

$d_{V90/10} = 2,79$

20um

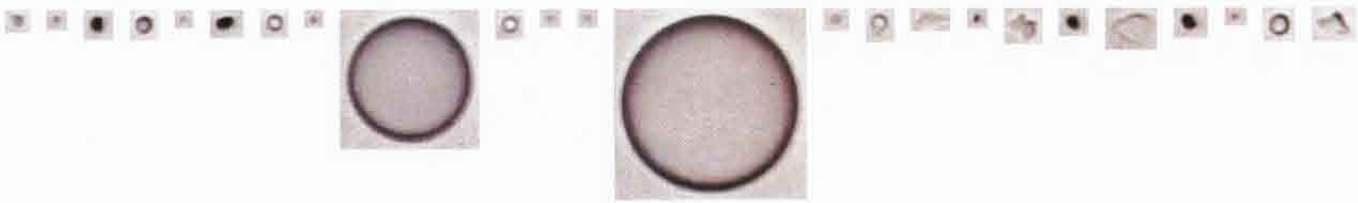

110314/042

FPIA-3000

Standard

10/03/2011

sysmex

Tested	
ReAnalyzed	10/03/2011 15:31:01
Measurer name	
ReAnalyzed By	Manager
SOP	
Sample name	XKR011_Merge
Sample number	1
Sample type	10 - 85 µm
Comment	9,1mg / 20ml
Power Field	LPF
Count method	Stop By Counts
Sheath Liquid	Particle Sheath

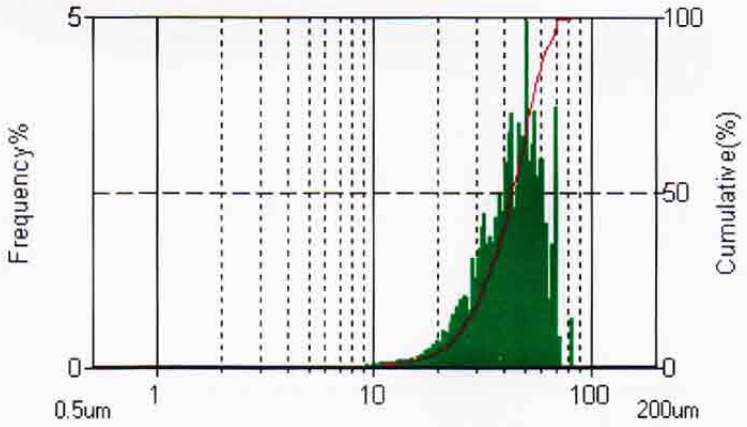

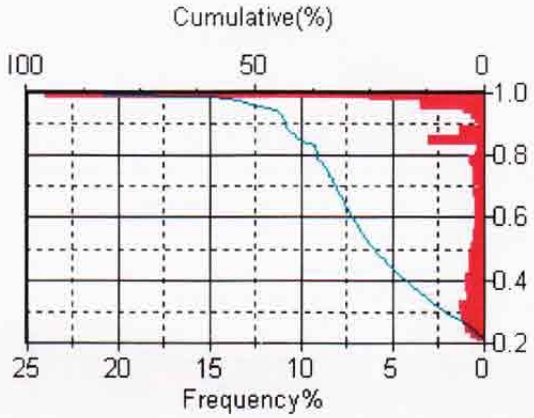

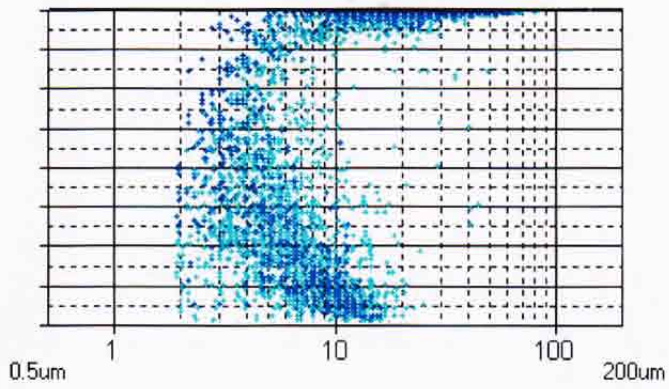

Particle dia

0.500 <= CE Diameter(V) < 200.0

Particle shap

0.200 <= Circularity <= 1.000

	CE Diameter(V)	Circularity		
Mean :	43.779	Mean :	0.784	Density : 121
SD :	14.192	SD :	0.273	Large(%) : 0.00
CV :	32.42	CV :	34.84	Middle(%) : 100.00
Mode :	51.060	Mode :	0.995	Small(%) : 0.00
Lower% :	25.131	Lower% :	0.319	Selected(%) : 100.00
50% :	43.684	50% :	0.966	Analyzed(#) : 6000
Upper% :	62.257	Upper% :	1.000	Selected(#) : 5999

dv90/10 = 2,477

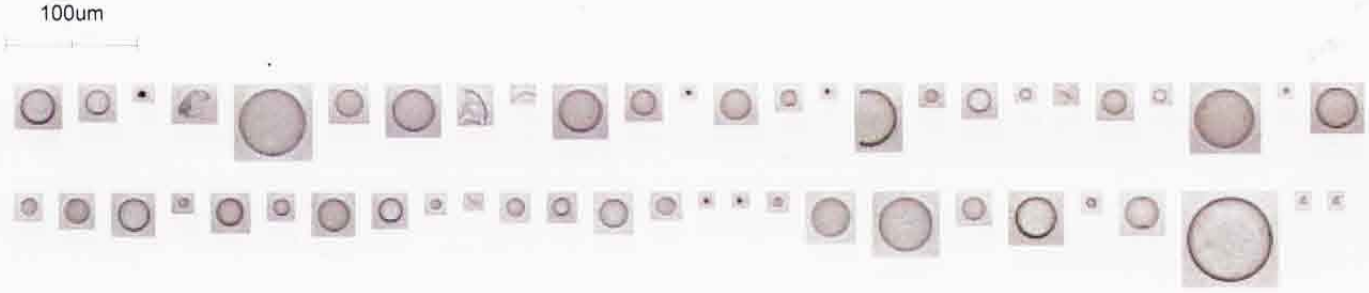

110310/UCA

FPIA-3000

Standard

26/05/2011

sysmex

Tested
ReAnalyzed 26/05/2011 12:30:09
Measurer name
ReAnalyzed By Manager
SOP
Sample name XKR019-71_MERGE
Sample number 1
Sample type
Comment
Power Field LPF
Count method Stop By Counts
Sheath Liquid Particle Sheath

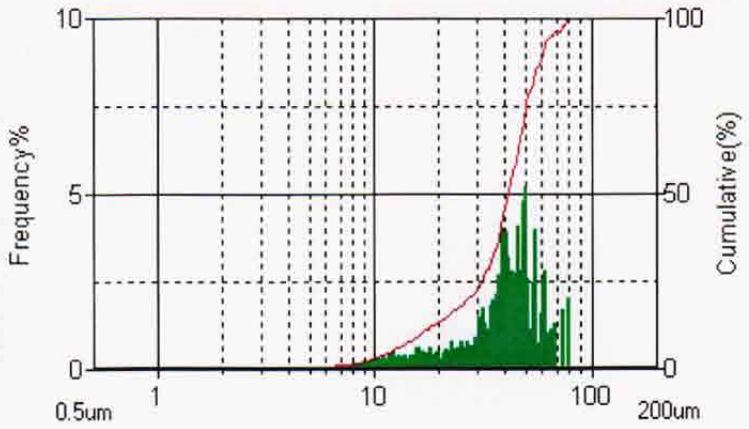

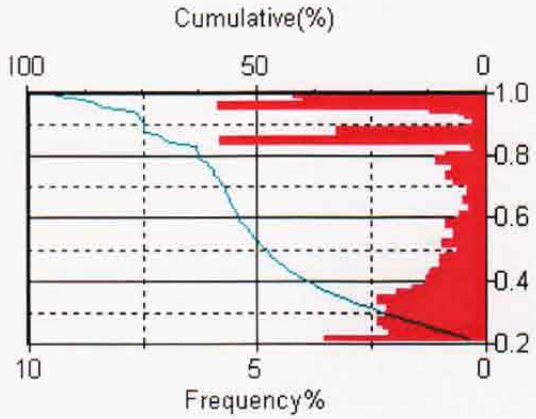

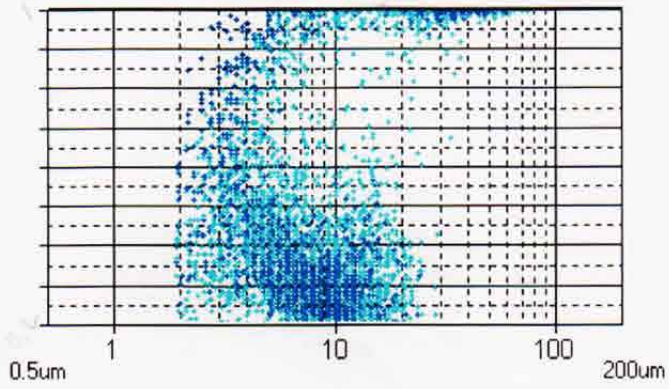

Particle dia

0.500 <= CE Diameter(V) < 200.0

Particle shap

0.200 <= Circularity <= 1.000

	CE Diameter(V)	Circularity		
Mean :	40.953	Mean :	0.600	Density : 69
SD :	16.024	SD :	0.293	Large(%) : 0.00
CV :	39.13	CV :	48.85	Middle(%) : 100.00
Mode :	49.724	Mode :	0.955	Small(%) : 0.00
Lower% :	16.506	Lower% :	0.247	Selected(%) : 100.00
50% :	41.724	50% :	0.537	Analyzed(#) : 6000
Upper% :	59.891	Upper% :	0.989	Selected(#) : 6000

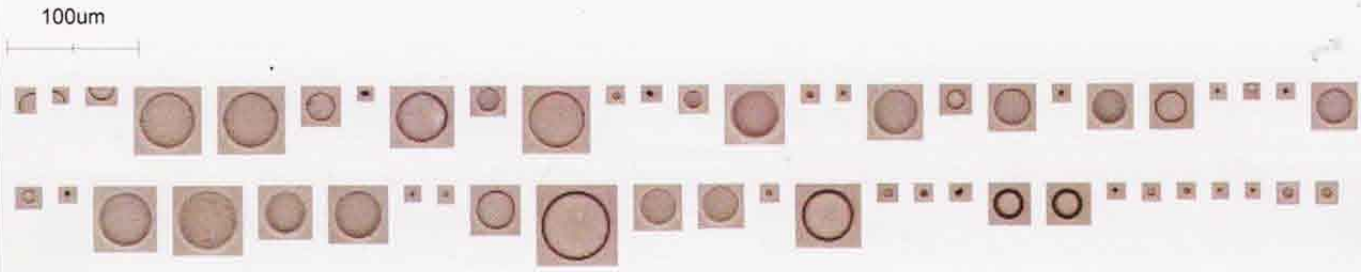

FPIA-3000

Standard

11/03/2011

sysmex

Tested	
ReAnalyzed	11/03/2011 13:41:23
Measurer name	
ReAnalyzed By	Manager
SOP	
Sample name	XKR010_Merge
Sample number	1
Sample type	10 - 60 µm
Comment	5,0mg / 20ml
Power Field	LPF
Count method	Stop By Counts
Sheath Liquid	Particle Sheath

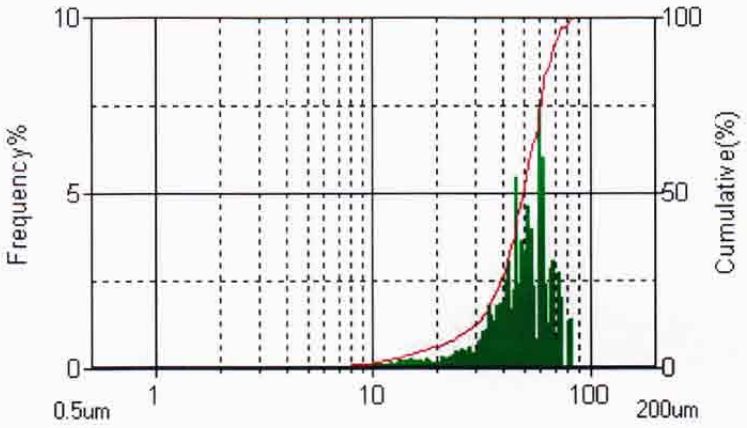

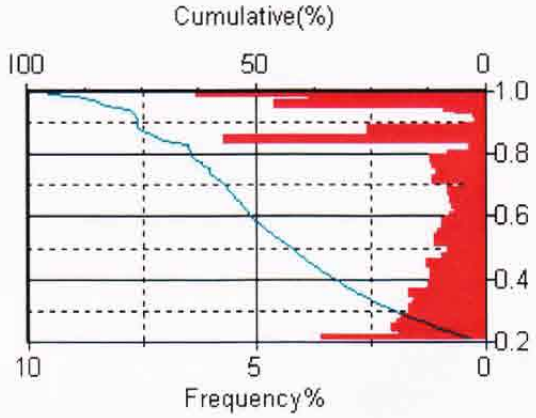

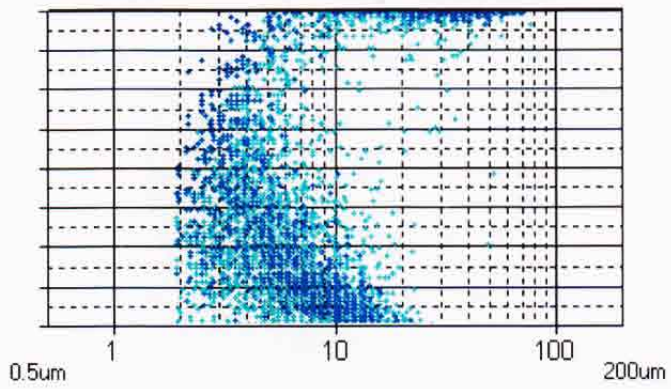

Particle dia

0.500 <= CE Diameter(V) < 200.0

Particle shap

0.200 <= Circularity <= 1.000

	CE Diameter(V)	Circularity		
Mean :	48.873	Mean :	0.615	Density : 74
SD :	16.083	SD :	0.282	Large(%) : 0.00
CV :	32.91	CV :	45.89	Middle(%) : 100.00
Mode :	58.298	Mode :	0.995	Small(%) : 0.00
Lower% :	26.621	Lower% :	0.248	Selected(%) : 100.00
50% :	49.925	50% :	0.592	Analyzed(#) : 6000
Upper% :	68.512	Upper% :	0.992	Selected(#) : 6000

$d_{V90/10} = 2,57$

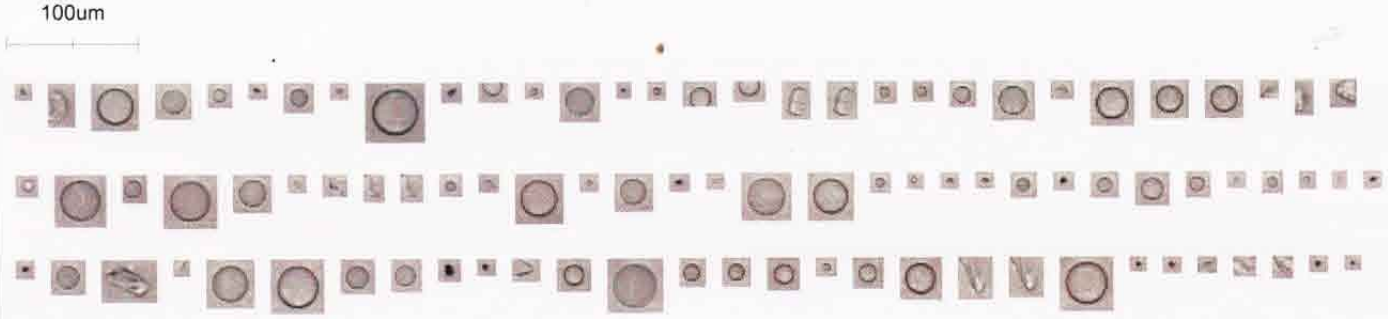

110314/UCA

FPIA-3000

Standard

24/05/2011

sysmex

Tested	
ReAnalyzed	24/05/2011 14:11:25
Measurer name	
ReAnalyzed By	Manager
SOP	
Sample name	XKR018_Merge
Sample number	2
Sample type	
Comment	5.0mg / 20ml
Power Field	LPF
Count method	Stop By Counts
Sheath Liquid	Particle Sheath

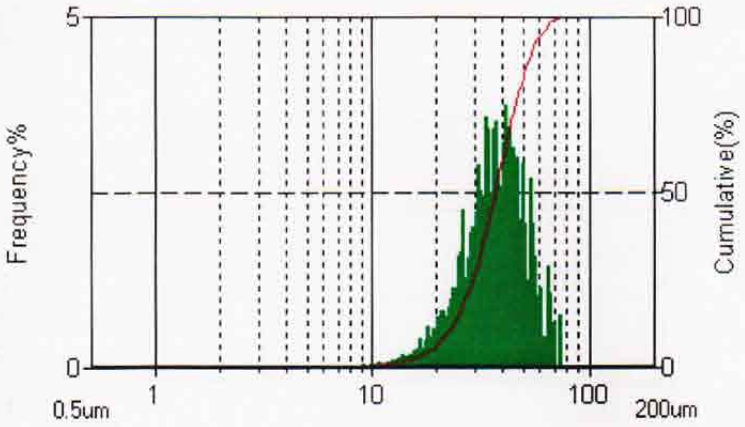

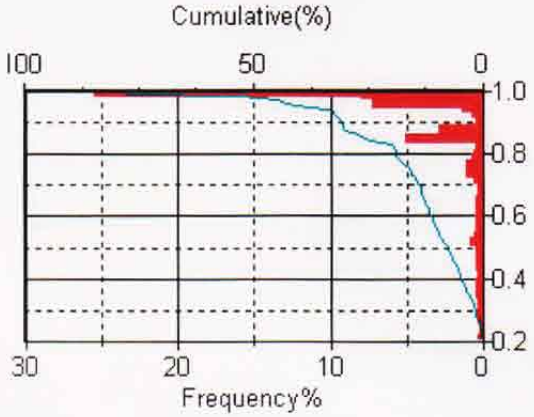

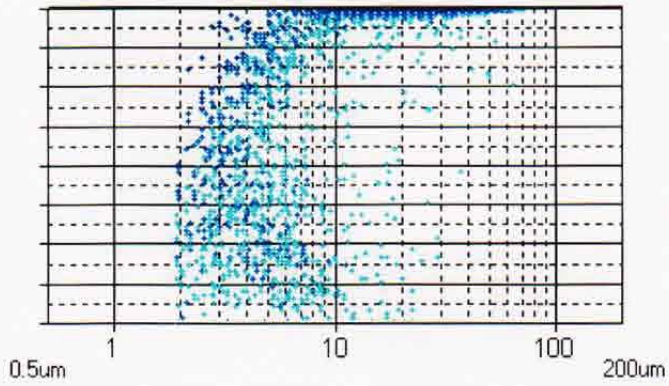

Particle dia

0.500 <= CE Diameter(V) < 200.0

Particle shap

0.200 <= Circularity <= 1.000

	CE Diameter(V)	Circularity		
Mean :	38.053	Mean :	0.889	Density : 92
SD :	12.613	SD :	0.186	Large(%) : 0.00
CV :	33.15	CV :	20.98	Middle(%) : 100.00
Mode :	41.302	Mode :	0.995	Small(%) : 0.00
Lower% :	22.617	Lower% :	0.562	Selected(%) : 100.00
50% :	36.990	50% :	0.989	Analyzed(#) : 6000
Upper% :	54.837	Upper% :	1.000	Selected(#) : 6000

dv90/10 = 2,42

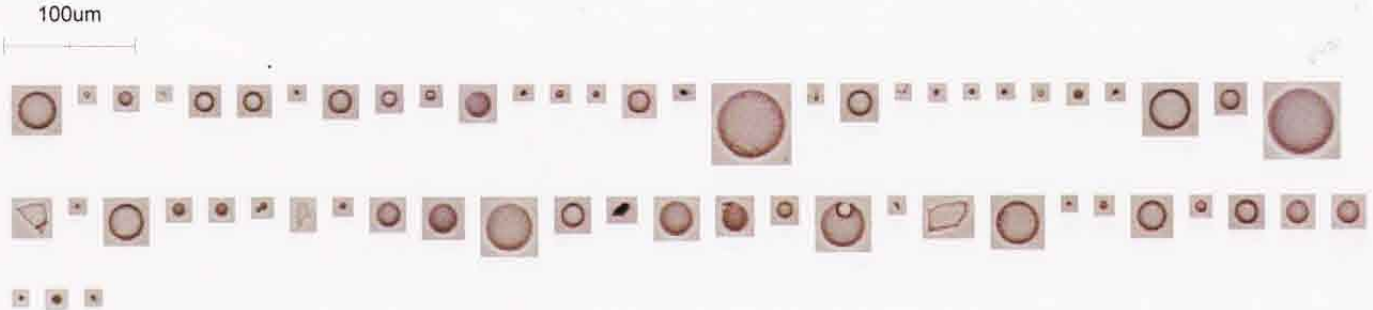

110524/UCA

FPIA-3000

Standard

19/05/2011

sysmex

Tested	
ReAnalyzed	19/05/2011 13:03:51
Measurer name	
ReAnalyzed By	Manager
SOP	
Sample name	XKR016_MERGE
Sample number	1
Sample type	
Comment	
Power Field	LPF
Count method	Stop By Counts
Sheath Liquid	Particle Sheath

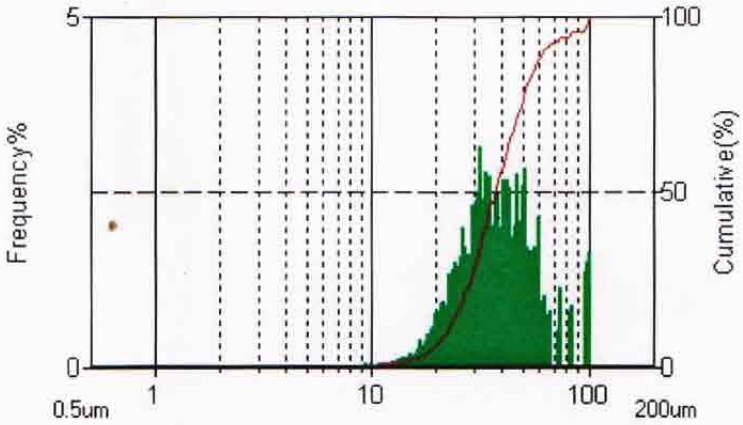

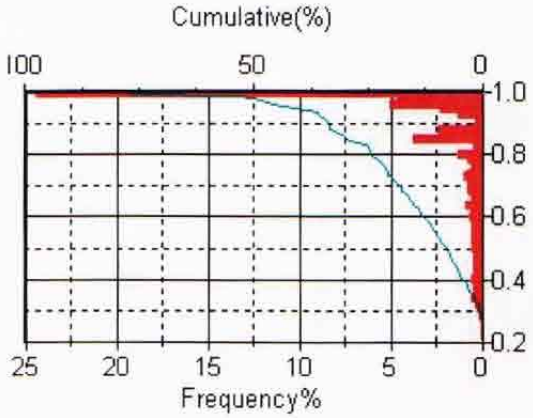

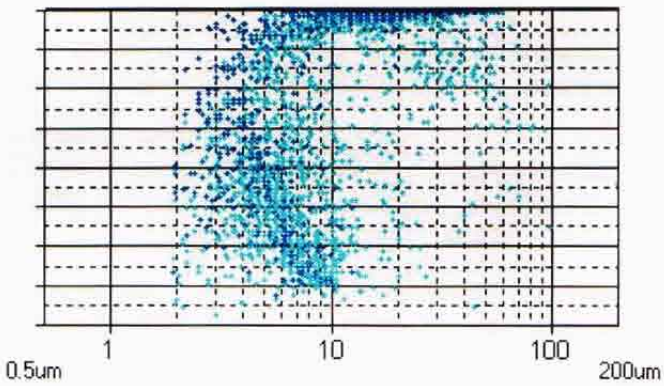

Particle dia

0.500 <= CE Diameter(V) < 200.0

Particle shap

0.200 <= Circularity <= 1.000

	CE Diameter(V)	Circularity		
Mean :	41.429	Mean :	0.875	Density : 42
SD :	19.055	SD :	0.189	Large(%) : 0.00
CV :	45.99	CV :	21.61	Middle(%) : 100.00
Mode :	31.684	Mode :	0.995	Small(%) : 0.00
Lower% :	22.331	Lower% :	0.548	Selected(%) : 100.00
50% :	37.406	50% :	0.985	Analyzed(#) : 6525
Upper% :	63.282	Upper% :	1.000	Selected(#) : 6525

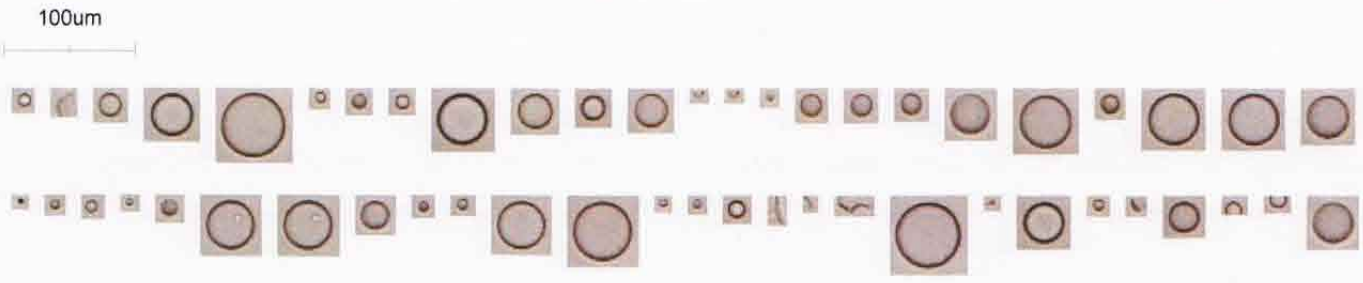

110519 /EO

FPIA-3000

Standard

22/03/2011

sysmex

Tested	
ReAnalyzed	22/03/2011 12:25:27
Measurer name	
ReAnalyzed By	Manager
SOP	
Sample name	XKR013_MERGE
Sample number	1
Sample type	2-30μM
Comment	
Power Field	HPF
Count method	Stop By Counts
Sheath Liquid	Particle Sheath

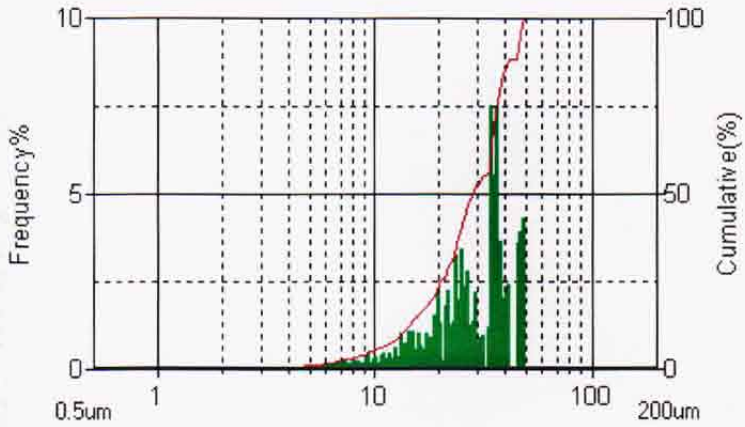

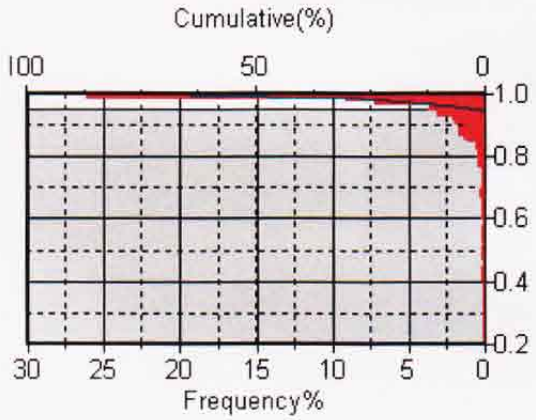

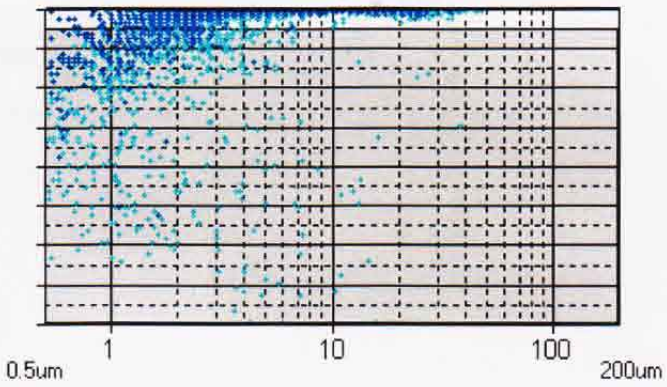

Particle dia

0.500 <= CE Diameter(V) < 200.0

Particle shap

0.950 <= Circularity <= 1.000

	CE Diameter(V)	Circularity		
Mean :	28.885	Mean :	0.991	Density : 324
SD :	11.280	SD :	0.013	Large(%) : 0.00
CV :	39.05	CV :	1.28	Middle(%) : 100.00
Mode :	36.175	Mode :	1.000	Small(%) : 0.00
Lower% :	13.438	Lower% :	0.971	Selected(%) : 96.10
50% :	28.914	50% :	0.996	Analyzed(#) : 6000
Upper% :	45.914	Upper% :	1.000	Selected(#) : 4144

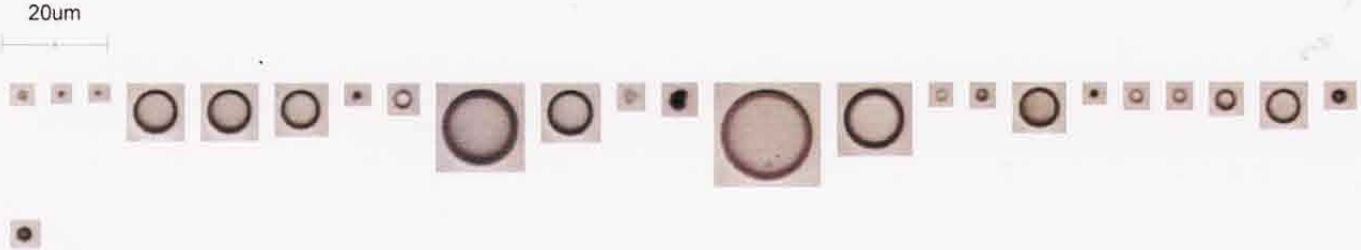

110322/EO

FPIA-3000

Extend5

14/03/2011

sysmex

Tested	
ReAnalyzed	10/03/2011 14:59:40
Measurer name	
ReAnalyzed By	Manager
SOP	
Sample name	XKR012_Merge
Sample number	1
Sample type	<2,5 - 10 µm
Comment	5,1mg / 20ml
Power Field	HPF
Count method	Stop By Counts
Sheath Liquid	Particle Sheath

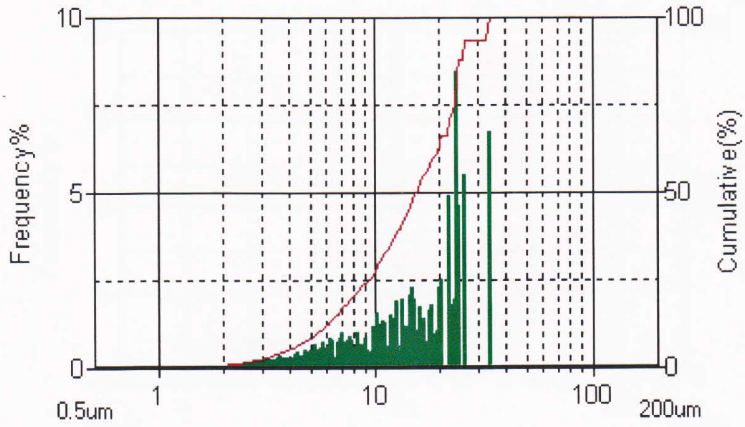

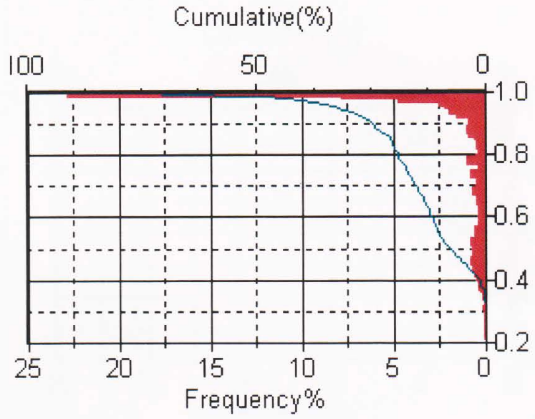

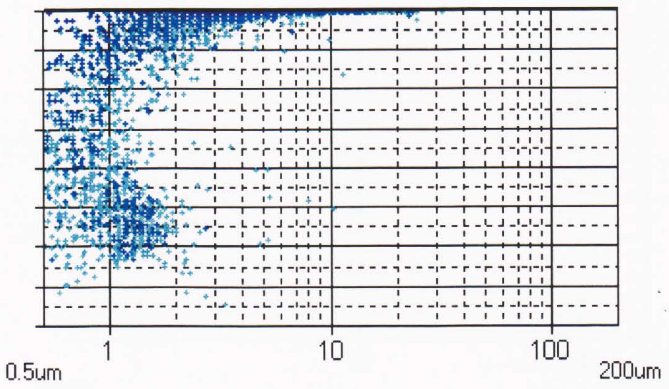

Particle dia

--- <= CE Diameter(V) < 200.0

Particle shap

--- <= Circularity <= ---

	CE Diameter(V)	Circularity		
Mean :	16.172	Mean :	0.900	Density : 3922
SD :	8.326	SD :	0.175	Large(%) : ******
CV :	51.48	CV :	19.48	Middle(%) : ******
Mode :	23.670	Mode :	1.000	Small(%) : ******
Lower% :	5.401	Lower% :	0.550	Selected(%) : 100.00
50% :	15.368	50% :	0.992	Analyzed(#) : 6000
Upper% :	25.483	Upper% :	1.000	Selected(#) : 5377

dv90/10 = 4,72

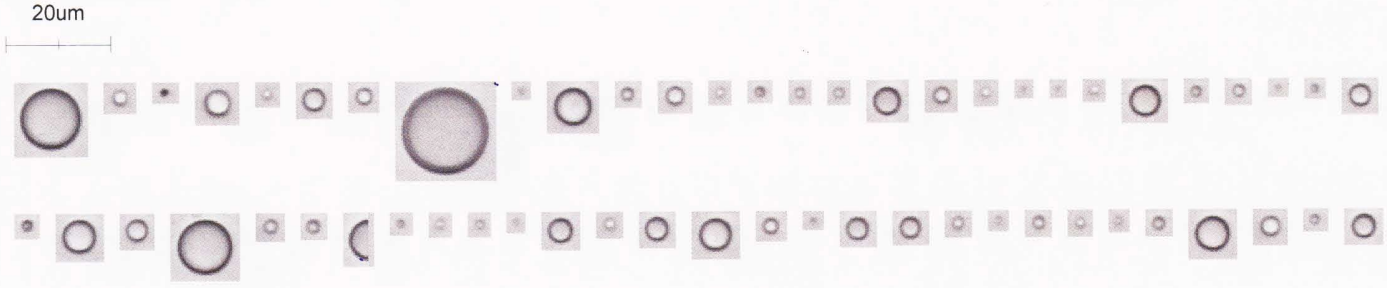

110314/UCA

FPIA-3000

Standard

31/03/2011

sysmex

Tested	
ReAnalyzed	31/03/2011 13:33:46
Measurer name	
ReAnalyzed By	Manager
SOP	
Sample name	XKR014_MERGE
Sample number	1
Sample type	
Comment	
Power Field	HPF
Count method	Stop By Counts
Sheath Liquid	Particle Sheath

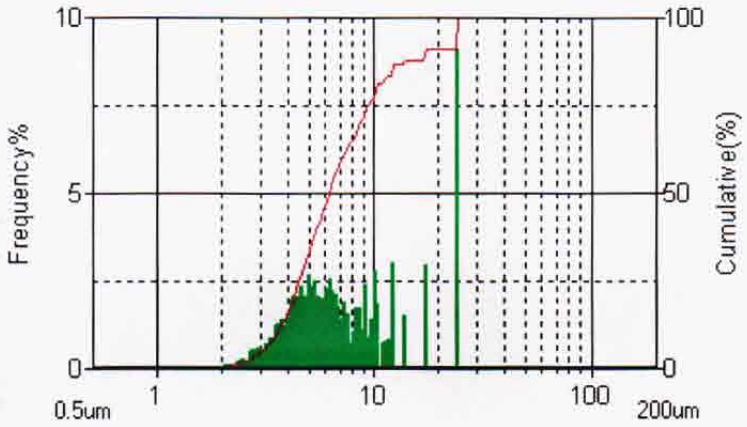

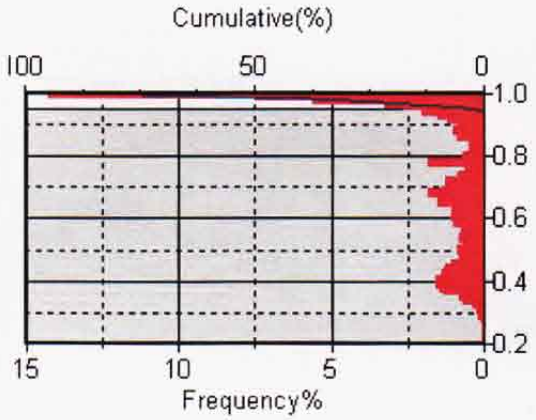

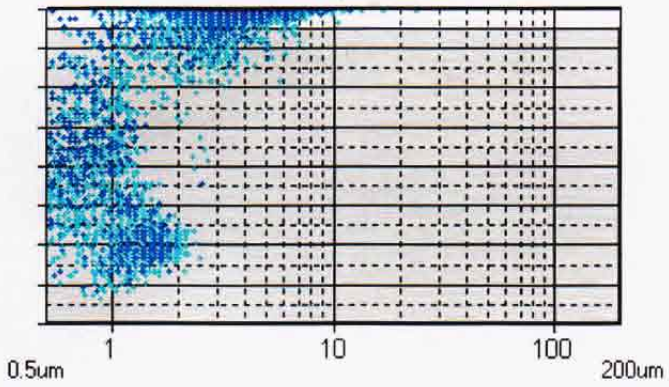

Particle dia

0.500 <= CE Diameter(V) < 200.0

Particle shap

0.950 <= Circularity <= 1.000

	CE Diameter(V)	Circularity		
Mean :	8.270	Mean :	0.988	Density : 4100
SD :	5.842	SD :	0.013	Large(%) : 0.00
CV :	70.64	CV :	1.37	Middle(%) : 100.00
Mode :	24.305	Mode :	0.995	Small(%) : 0.00
Lower% :	3.554	Lower% :	0.966	Selected(%) : 91.92
50% :	6.241	50% :	0.993	Analyzed(#) : 6000
Upper% :	17.093	Upper% :	1.000	Selected(#) : 2168

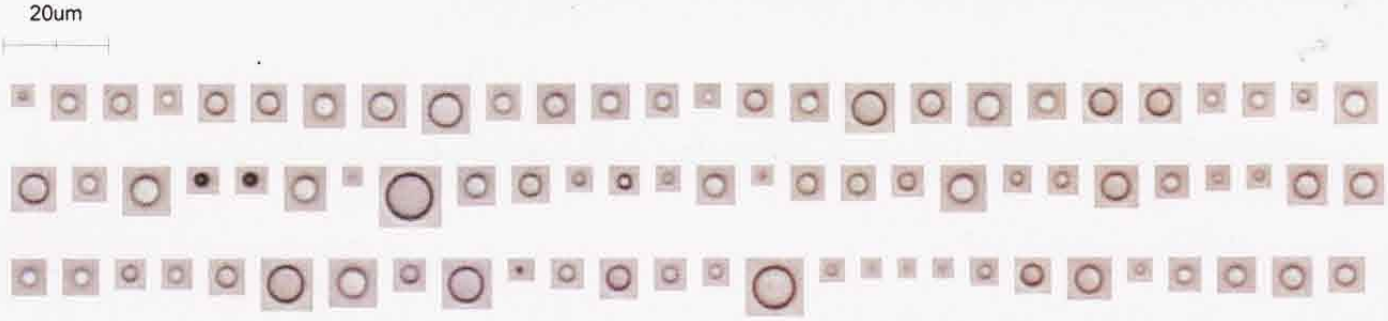

110331 /EO

FPIA-3000

Standard

18/05/2011

sysmex

Tested	
ReAnalyzed	18/05/2011 10:55:05
Measurer name	
ReAnalyzed By	Manager
SOP	
Sample name	XKR017_merge
Sample number	1
Sample type	~2μm fraktion
Comment	
Power Field	HPF
Count method	Stop By Counts
Sheath Liquid	Particle Sheath

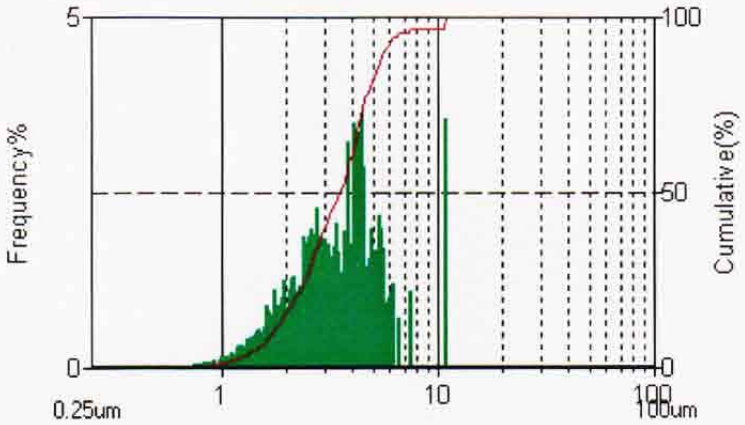

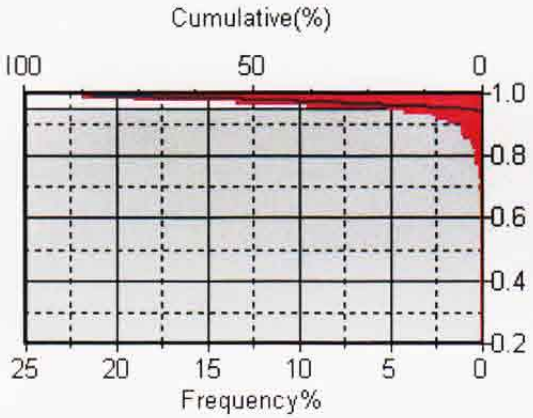

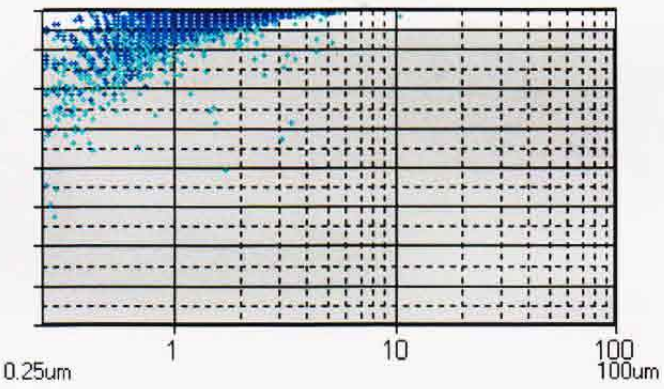

Particle dia

0.250 <= CE Diameter(V) < 100.0

Particle shap

0.950 <= Circularity <= 1.000

	CE Diameter(V)	Circularity		
Mean :	3.785	Mean :	0.984	Density : 40214
SD :	1.978	SD :	0.013	Large(%) : 0.00
CV :	52.26	CV :	1.36	Middle(%) : 100.00
Mode :	4.438	Mode :	0.995	Small(%) : 0.00
Lower% :	1.737	Lower% :	0.964	Selected(%) : 97.24
50% :	3.525	50% :	0.987	Analyzed(#) : 6000
Upper% :	5.661	Upper% :	1.000	Selected(#) : 4535